

1 To: Associate Editor, Jochen Schöngart

2

3 Dear Editor,

4

5 Thank you for handling this manuscript. We are pleased to see that the feedback from the  
6 reviewers was overall positive, and that they both suggested improvements to the manuscript,  
7 which we took onboard.

8 Both reviewers pointed out issues with the calibration of our new model (henceforth referred to  
9 as LCA model). Our methodology was not clearly stated. The LCA model was not calibrated  
10 from Lidar data but from ground data at 4 sites, and we edited the manuscript to avoid confusion  
11 about it. We developed the local models based on MCH to confirm the optimal height threshold  
12 for segmentation as indicated by Figure 2 and Figure 3. MCH-inferred AGB values are now just  
13 used as a test for validation of our height threshold in Figure 3. We also added sections  
14 comparing the LCA model to a similar model based on MCH calibrated from the same 4 sites, as  
15 suggested by the reviewers.

16 Comments made by both reviewers were addressed in the authors' comments as part of the  
17 interactive discussion process, and are presented here again, with additional information about  
18 changes that were made in the manuscript.

19 Please note that all references to changes in manuscript correspond to the line numbers of the  
20 revised manuscript with track changes.

21 We believe that these changes and the ones described below improved the clarity of our paper,  
22 and that it is now acceptable for publication in your journal.

23

24 Sincerely,

25

26 Victoria Meyer, on behalf of all co-authors.

27

28 **Response to Anonymous Referee #1**

29

30 **Response to General comments:**

31

32 Thank you for reviewing our manuscript. We greatly appreciate your comments and did our best  
33 to address the issues you brought up. Your comments highlighted the fact that our methodology  
34 was not clearly stated. The LCA model was calibrated using inventory data from the four sites  
35 referred to as “calibration sites” in the manuscript. Based on both reviews of the paper, we  
36 decided to remove Figure 5b and moved the paragraph explaining how  $AGB_{Lidar}$  (renamed  
37  $AGB_{Local}$  for clarity) was calculated to the Supplementary Information (S.2), to make the paper  
38 more straight forward and focused on LCA.  $AGB_{Local}$  values are now just used as a test for  
39 validation of our height threshold in Figure 3.

40

41

42 **Comment:** “In the methods section, it is unclear whether they are predicting  $AGB_{Lidar}$  and  
43  $AGB_{LCA}$  from an equation that already exists or whether they are doing a regression analysis  
44 to find values for parameters ‘a’ and ‘b’ in Eqs. 1-3. If it’s the former, show the actual values for  
45 ‘a’ and ‘b’.”

46 **Response:** The form of Equation 1 (now Equation S4) is a commonly used model form to  
47 estimate AGB from Lidar locally (see Asner and Mascaro, 2014). For each site (or group of sites  
48 for Manaus, Tapajos and Cotriguaçu), we performed a regression based on that form and  
49 obtained coefficients a and b, presented in Table S1 (SI, ls.50-51: “All coefficients are presented  
50 in Table S1”).

51 We decided to move this section to the Supplementary Information, as it is not central to the  
52 paper and is just used to obtain Figure 3a in this new version of the paper.

53 Coefficients a and b for Equation 2) and 3) (now Eq 1 and 2) are presented in Table 3. We added  
54 a sentence that makes a clear reference to the coefficients in that table. Also, we moved the  
55 section presenting the form of the LCA models from the Methods to the Results section, for  
56 clarity (ls.358-364).

57 **Changes to manuscript:** ls.334-335 “The coefficients of the models, as well as their respective  
58 coefficients of correlation, RMSE and bias from all training data and cross-validation are  
59 reported in Table 3.”

60

61 **Comment:** “Either way, it doesn’t seem necessary to predict AGB from MCH other than to  
62 compare AGB estimates from LCA to those from MCH (eg, show improvement in new  
63 method).”

64 **Response:** Based on both reviewers’ comments, we removed the part of the analysis that  
65 compared  $AGBLCA$  to the locally estimated  $AGB_{Lidar}$ . As a result, Figure 5b was removed.  
66 Instead, we are now comparing AGB estimations from LCA and MCH based on the same  
67 methodology: in both cases, models were fitted using the field  $AGB_{inv}$  of the four calibration  
68 plots. This is presented in the Methods (ls.218-240), in the Results (ls. 345-379) and in the  
69 Discussion (ls.563-569).

70 **Changes to manuscript:** see ls. 218-240, ls. 345-379 and ls. 563-569. Figure 5

71

72 **Comment:** “In section 2.3 the authors say they have only 4 calibration sites (instead of 9 in the  
73 abstract).”

74 **Response:** We realize that the abstract was misleading. We added a sentence stating that the  
75 model was calibrated using 4 sites. We also removed the word “nine” in the title of the paper.  
76 Changes to manuscript: ls.45-46: “...and ground inventory data in nine undisturbed old growth  
77 Neotropical forests, of which four had plots large enough (1ha) to calibrate our model.”

78

79 **Comment:** “So, is AGB in the other five sites predicted by Eq 1 (MCH)?”

80 **Response:** AGB<sub>LCA</sub> in the other sites was estimated using the same LCA model calibrated from  
81 the 4 calibration sites (Eq 2). AGB<sub>MCH</sub> was calculated using the MCH model presented in Table  
82 S3.

83

84 **Comment:** “I suggest the authors remove AGB\_Lidar estimates and focus on relating LCA  
85 metrics to AGB determined from ground inventories.”

86 **Response:** Thank you for your suggestion. We removed figure 5b and removed the paragraphs  
87 related to AGB<sub>Lidar</sub> in Section 2.2. The information on AGB<sub>Lidar</sub> (renamed as AGB<sub>Local</sub>) are now  
88 provided in the Supplementary Information (S.2). AGB<sub>Local</sub> is now only used to provide  
89 additional information on the choice of the height threshold in Figure 3. (nb: equation numbers  
90 have changed).

91 We edited the text to emphasize the role of the calibration plots and show that AGB<sub>Local</sub> was just  
92 used as an additional/confirmation step.

93 **Changes to manuscript:** ls.200-206: “We determined the optimal minimum canopy height  
94 threshold calculating the coefficient of correlation between AGB<sub>inv</sub> and LCA at the four  
95 calibration sites. (...). We also estimated AGB from Lidar data locally (AGB<sub>Local</sub>) using a  
96 commonly used model fit relating MCH to AGB<sub>inv</sub> in each site, to further examine the variations  
97 of LCA and AGB in all nine sites (see S.2, Table S1).”

98

99 **Comment:** “Furthermore, I suggest trying to optimize AGB estimates from LiDAR by, for  
100 example, estimating AGB with both LCA and MCH.”

101 **Response:** We tested different model forms for Equation 2 and 3 (now Equations 1 and 2),  
102 including models using both LCA and MCH as predictors. Using MCH in addition to LCA did  
103 not improve the performance of the model. This is stated in the sentence ls.234-237 “We tested  
104 different models to infer AGB<sub>inv</sub> from LCA, henceforth called AGB<sub>LCA</sub>, at the four calibration  
105 sites, and explored if adding more parameters, such as mean wood density of a site, mean wood  
106 density of large trees (DBH ≥50 cm), mean canopy height or top percentiles of canopy height  
107 improved the predicting power of the model.” We added:

108 **Changes to manuscript:** ls.311-331 “Adding more parameters did not improve the performance  
109 of the model, except when using WD as a normalizing factor. The two models we retained are  
110 therefore of the form of Eq. (1) and Eq. (2)”

111

112 **Responses to specific comments:**

113 **Comment:** How is the LCA method weighted by WD if there isn’t ground data at 5 sites?

114 **Response:** Ground data are available in all sites except Cotriguaçu, but plot size was too small to  
115 be used in the LCA model calibration process. However, wood density estimation does not  
116 depend on plot size, and wood density information was used from all sites to obtain a site-  
117 averaged wood density (see Table 1). A sentence was added to highlight this point:

118 **Changes to manuscript:** ls.138-145: “For this reason, all plots smaller than 1 ha were excluded  
119 from the LCA analysis but were used in estimating average wood density for each site, which  
120 does not depend on plot size. Stand averaged wood density was calculated based on the wood  
121 density of all trees present in a site, determined using the commonly used global wood density  
122 database, and is reported in Table 1 (Chave et al., 2009; Zanne et al., 2009). For Cotriguaçu, we  
123 used stand averaged wood density given by Fearnside, (1997) for a region covering the site.”

124  
125 **Comment:** Line104: what do you mean by ‘unique’?

126 **Response:** by “unique”, we mean one model that would work across sites in the Neotropics.

127 **Changes to manuscript:** l.112: We modified the sentence accordingly to “single”.

128

129 **Comment:** Line 166: What model? Line 167: what data?

130 **Response:** The text was edited to clarify this sentence.

131 **Changes to manuscript:** SI, ls.55-58 “For the remaining sites of the Central Amazon  
132 (Cotriguaçu, Manaus and Tapajós), we developed a model based on existing data in Manaus and  
133 Tapajós from a previous study, derived from airborne and spaceborne Lidar (see Lefsky et al.,  
134 2007).” Note that this section is now part of the Supplementary Information, as explained above.

135

136 **Comment:** Lines 203-4: This indicates that AGB\_LCA is being tested against AGB\_Lidar,  
137 where LiDAR is being treated as the reference. AGB\_Lidar is only an estimate.

138 **Response:** This is correct. The goal here was to test  $AGB_{LCA}$  against locally derived  $AGB_{Lidar}$ .  
139 Based on both reviewers’ comments, we realized that this step was not necessary and was  
140 removed from the paper.

141 **Changes to manuscript:** Figure 5b and any text related to this graph were removed from the  
142 paper.

143

144 **Comment:** Lines 205-6: Here you say that these results were compared to ‘a traditional model  
145 relying on MCH to estimate AGB’. Isn’t AGB\_Lidar the model relying on MCH to estimate  
146 AGB?

147 **Response:** Thank you for highlighting this point. Here, we refer to a single model based on  
148 MCH from all the calibration sites, the same way that the LCA model was calibrated. This way,  
149 we can compare the LCA model to a MCH model. We realize that this sentence is confusing and  
150 edited the manuscript to clarify it: as stated above,  $AGB_{Lidar}$  is now only used to obtain Figure 3b  
151 and is no longer compared to  $AGB_{LCA}$ . Instead, we added a new section in the methods, results  
152 and discussions comparing  $AGB_{LCA}$  and  $AGB_{MCH}$  (based on a model calibrated on the same 4  
153 calibration sites). Please report to our response to earlier comment.

154

155 **Comment:** Section 2.5: Is it possible to apply the same methods to logged areas, since you may  
156 not know which areas have been harvested or not – or have before and after pictures?

157 **Response:** We agree that we need before-after data to detect logging. In the example we are  
158 showing, we do have before and after logging Lidar data. Details are provided in Anderson et al.,  
159 2014.

160 We added a sentence to emphasize on the need for this type of datasets.

161 **Changes to manuscript:** ls.246-247: “provided that Lidar data are available from pre and post-  
162 logging.”

163

164 **Comment:** Line 269: Where did wood volume data come from?  
165 **Response:** we edited the manuscript to clarify this point:  
166 Changes to manuscript: ls.307-309: “Since AGB depends on DBH, H and WD (see Chave et al.,  
167 2014), average wood volume can be computed approximately as the ratio of AGB divided by the  
168 average wood density”.

169  
170 **Comment:** Lines 315-6: In what way does Antimary not represent Peruvian Amazon and  
171 Amazon-Andes gradients?  
172 **Response:** We added the following sentence to be more specific :  
173 **Changes to manuscript:** ls.418-421: “However, this site does not represent forests in the  
174 western Amazon or the Amazon-Andes gradients with relatively lower wood density (Baker et  
175 al. 2004) and more fertile volcanic soils impacting the forest structure and dynamics (Quesada et  
176 al., 2011).”

177  
178 **Comment:** Line 323: by how much does it explain the variation?  
179 **Response:** Overall 78% is explained ( $R^2=0.78$ ).  
180 **Changes to manuscript:** l.428: “and explained 78% of the variation”.

181  
182 **Comment:** Section 4.3: Would be helpful to refer to tables and figures  
183 **Response:** Thank you for the suggestion. We added references to table 2 and figure 3.  
184 Changes to manuscript: references l.465 and l.468.

185  
186 **Comment:** Lines 344-6: This sentence is unclear to me, but it sounds like it supports my point  
187 that using AGB\_Lidar as a reference is circular and not proving anything  
188 **Response:** This sentence was not clear and was removed from the manuscript. Moreover, we are  
189 now comparing AGB from LCA and MCH in a separate section of the results and discussion to  
190 avoid any confusion.

191  
192 **Comment:** Line 374: Change ‘only’ to ‘primarily’ or something similar.  
193 **Response:** “only” was removed.

194  
195 **Comment:** Line 391: Change ‘Any’ to ‘Most’  
196 **Response:** We changed “‘Any’ to ‘Most’.

197  
198 **Comment:** Lines 423-5: Maybe the relationship is not linear at the high end of LCA  
199 **Response:** It is indeed a possibility. We added this suggestion to the manuscript.  
200 Changes to manuscript: ls. 589-591: “It is also possible that the relationship between AGB and  
201 LCA is not linear for very high AGB values. This could be tested in the future with a larger  
202 number of sites with very high biomass.”

203  
204 **Comment:** Line 467: If the relationship remains unique across forest types, is it not then broadly  
205 applicable?  
206 **Response:** Yes, this is an important point of the paper. We added two sentences highlighting this  
207 fact.  
208 **Changes to manuscript:**  
209 - in the Discussion:

210 ls.538-539: “Our model can therefore potentially be applied to a wide range of forest types,  
211 provided that there is information about wood density of the study area in the literature.”  
212 - in the Conclusion:  
213 ls.640-641: “. This linear relationship remains unique across different forest types, making the  
214 LCA model broadly applicable.”

215  
216 **Comment:** Fig 3: Clever way to find the optimal H threshold

217 **Response:** Thank you for this positive comment.

218

219 **Comment:** Fig 4b: This doesn't look like a perfectly fit.

220 **Response:** With a R2 of 0.78, RMSE of 46 and no bias, we consider the fit to be good. These  
221 number are provided in Table 3. R2 was added to Figure 4b to emphasize this point.

222 **Changes to manuscript:** R2 was added to Figure 4b to emphasize this point.

223

224 **Comment:** Fig 5b: All calibration sites are above the 1:1 line. Why are Nouragues and Choco  
225 below the line?

226 **Response:** Based on your comments and that of Reviewer 2, we removed this figure. The fact  
227 that some plots were above/below the line was likely due to the fact that  $AGB_{Lidar}$  was estimated  
228 locally for different sites and included some error. We are now simply comparing the LCA and  
229 MCH methods based on the inventory data only (Figure 5, attached here as Fig.1).

230

231 **Comment:** Fig 7: It would be helpful to see the actual data, not just regression lines.

232 **Response:** The point of this figure is to clearly see where the lines cross the y axis. For Fig 7a),  
233 we are just showing where the LCA model crosses the y axis, with different wood density from  
234 the different sites. Each line represents the model curve with various wood density values. To see  
235 the actual data from the calibration sites, see Figure 4b.

236 For fig 7b, actual data could be added, but just showing the lines gives the figure a clean look,  
237 considering that the information we are looking for here is the intercept of each line.

238

239

## 240 **Response to Anonymous Referee #2**

241

242 Thank you for taking the time to review our paper. We did our best to address all your comments  
243 in the hope this will improve the quality of the manuscript.

244

245 **Comment:** For this method to be useful, it must either (1) outperform existing methods, (2)  
246 perform similarly to existing methods but at lower computational cost or (3) open up new  
247 applications not allowed by existing methods.

248

249 **Response :** Our study does open up new applications compared with existing methods. We  
250 demonstrate that our method performs similarly to another method relying on information from  
251 all trees within a plot (MCH). The point of our paper is not to say that the LCA method is better  
252 than the MCH method, but rather to show that information on large trees is enough to estimate  
253 biomass. Our findings confirm what has been shown in several studies focusing on ground data  
254 (Bastin et al, Slik et al...) and shows for the first time that relying on large trees from a remote

255 sensing perspective allows to estimate AGB. It opens up new applications both for field  
256 inventory and remote sensing applications. In the discussion (section 4.8), we talk about how  
257 methods focusing on large trees could help future space missions, such as BIOMASS and GEDI,  
258 to accurately estimate biomass and open up new applications. LCA also gives information on the  
259 presence of large trees in a study area, which other metrics such as MCH cannot do. It is an  
260 important point, considering that large trees are often the most affected by natural disturbance  
261 and targeted by logging companies.

262 **Changes to manuscript:** ls.455-457: “LCA provides information on the presence of large trees  
263 in a study area, which other metrics such as MCH cannot do. It is an important point, considering  
264 that large trees are often the most affected by natural disturbance and targeted by logging  
265 companies.”

266 ls.564-565: “The comparison of LCA and MCH metrics showed that both performed similarly in  
267 estimating AGB, highlighting the importance of large canopy trees to estimate biomass.”

268 ls.645-647: “The results of our study may encourage further research in the use of Lidar data for  
269 detecting the distribution of larger trees in tropical forests for ecological and conservation  
270 studies.”

271  
272 **Comment:** The paper is framed around comparing the new LCA method against the existing  
273 MCH method, but a clear comparison of the two against ground-based validation data is not  
274 presented.

275  
276 **Response:** Thank you for pointing this out. We added a short paragraph in the method section, as  
277 well as a new section in the Results and in the Discussion, comparing the performance of LCA  
278 and MCH methods. This is presented in the Methods (ls.218-240), in the Results (ls. 345-379)  
279 and in the Discussion (ls.563-569).

280 To avoid any confusion, we moved the MCH local estimations of AGB from the main Lidar data  
281 paragraph to the Supplementary information (S.2).  $AGB_{Lidar}$  was also renamed  $LCA_{Local}$  for  
282 clarity.

283 **Changes to manuscript:** see ls. 218-240, ls. 345-379 and ls. 563-569. Figure 5 (attached here as  
284 Fig. 1)

285 We chose to keep Table S3 in the Supplementary Information for clarity, but we added a figure  
286 comparing AGB estimations using the 2 methods (Figure 5).

287  
288 **Comment:** Is LCA quicker to calculate than MCH? It would be useful to present a comparison  
289 of the computational time taken to calculate LCA versus MCH.

290  
291 **Response:** LCA is not quicker to calculate than MCH, but it is not significantly slower either  
292 (below 1s for both methods). Also, the strength of LCA lies in the structural information it  
293 provides, not in its computational time. Thus, we chose not to add a detailed comparison of  
294 computational time.

295  
296 **Comment:** The application to detect the impacts of selective logging is potentially very  
297 important.

298  
299 **Response:** We agree. We emphasized this point in the Discussion:

300 **Changes to manuscript:** ls.609-611: “LCA could become an important tool to detect forest  
301 degradation, in particular selective logging, considering that large trees are targeted by logging  
302 companies.”

303  
304 **Comment:** My main suggestion to improve this paper are to concentrate on testing the relative  
305 performance of LCA and MCH approaches at estimating biomass when validated against  
306 inventory data (even if LCA performs worse, this is still a very useful result for method  
307 development),  
308

309 **Response:** Thank you for your suggestion. As mentioned above, we added a paragraph in the  
310 method section, as well as two new sections (results and discussion) and a figure comparing the  
311 two methods, showing that they perform very similarly. We also show how they differ in terms  
312 of AGB estimations in different sites.  
313

314 **Comment:** and comparing the performance of the two approaches when applied to detect the  
315 impacts of selective logging.  
316

317 **Response:** We compared the performance of the 2 approaches when applied to selective logging  
318 detection. The MCH model showed a loss of biomass of 19 Mg ha<sup>-1</sup>, compared to 15 with LCA  
319 and 9 from a previous study based on rh25. We added this information in the results and the  
320 discussion.

321 **Changes to manuscript:** ls.393-394: “As a comparison, the MCH model led to an estimated  
322 biomass loss of 19 Mg ha<sup>-1</sup>.”

323 ls.607-609: “The higher biomass loss estimation from the MCH model (19 Mg ha<sup>-1</sup>) again shows  
324 how different metrics can lead to different results. Here, three methods based on three different  
325 Lidar metrics yielded results that differed by more than twofold.”.  
326

327 **Comment:** I agree with reviewer 1 in that I don’t see much value in testing the performance of  
328 LCA against biomass estimates using MCH.  
329

330 **Response:** Thank you for your suggestion. We removed Figure 5b. Performance comparison of  
331 LCA and MCH model at the calibration sites is now based on Figure 5a. The models applied to  
332 the nine sites are now Figure 5b, following your other suggestion to focus on the comparison of  
333 LCA and MCH methods.

334  
335 **Specific comments:**  
336

337 **Comment:** Line 205 – How was bias calculated?  
338

339 **Response:** We added the definition of bias to the manuscript:

340 **Changes to manuscript:** ls.214-215: “bias (mean difference between the expected values of  
341 AGB and the observed values of AGB)”.

342  
343 **Comment:** Line 262 – What are the other models apart from a power law fit?  
344

345 **Response:** For both LCA and MCH models, we tested linear models and power laws, which are



346 the 2 common fits. We modified the sentence to avoid any confusion:  
347 **Changes to manuscript:** ls.302-303: “with a better coefficient of correlation and RMSE than a  
348 power law fit”  
349

350 **Comment:** Line 262 – 263 – Are RMSE values and r squared values here from cross-validation  
351 or from the training data? Line 263 – Just present the bias from cross-validation.  
352

353 **Response:** R<sup>2</sup> and RMSE are from training data.

354 We removed the bias from the training data and present the bias from cross-validation.

355 **Changes to manuscript:** l.304: “bias<sub>cross\_val</sub> = 0.16 Mg”

356 ls.334-336: “coefficients of correlation, RMSE and bias from training data and cross-validation  
357 are reported in Table 3.”  
358

359 **Comment:** Line 271 – How feasible is it to scale by wood density in the absence of inventory  
360 data? Presumably errors would be larger if modelled estimates of wood density were used.  
361

362 **Response:** We agree. If there is no information in the literature from previous studies, modelled  
363 WD could be used, but would indeed give greater errors. This is now covered in the Discussion.

364 **Changes to manuscript:** ls.558-561: “In the absence of information on wood density from the  
365 literature, modelled wood density could potentially be used, but would give greater errors. These  
366 errors should be taken into account when reporting on the uncertainty of the results.”  
367

368 **Comment:** Lines 287-301 – It would be useful to also see how MCH performs at detecting this  
369 loss of biomass.  
370

371 **Response:** The MCH model (Table S3) gives a biomass loss of 19mg/ha, more than twice what  
372 was reported in Andersen et al., 2014. These results were added to the results section and the  
373 discussion section 4.6.:

374 **Changes to manuscript:** ls.393-394: “As a comparison, the MCH model led to an estimated  
375 biomass loss of 19 Mg ha<sup>-1</sup>.”

376 ls.607-609: “The higher biomass loss estimation from the MCH model (19 Mg ha<sup>-1</sup>) again shows  
377 how different metrics can lead to different results. Here, three methods based on three different  
378 Lidar metrics yielded results that differed by more than twofold.”  
379

380 **Comment:** Lines 376-377 – This is a very nice approach to identify how much biomass is  
381 missed by LCA.  
382

383 **Response:** Thank you for this positive comment.  
384

385 **Comment:** Figure S2 - Given that the minimum cluster size didn't have a major effect on the  
386 AGB estimates, I would be interested in seeing a comparison of the performance of the LCA  
387 metric just following masking versus the LCA metric following removal of segments below the  
388 threshold cluster size. How computationally costly are these last steps?  
389

390 **Response:** This is a good point. For a reference image of 1000x1000m pixels, the full process  
391 takes less than one second. Just using masking may be slightly faster, but the computational cost

392 is not an issue here. Just using masking gives similar results as when using LCA, because the  
393 pixels removed by the full process represent a small fraction of the area covered by large trees  
394 (1.73% on average). ( $R^2=0.78$ ,  $RMSE=45.7$ ,  $bias=0.55$ )  
395 These isolated pixels either represent single branches reaching above 27m or the tip of a tree  
396 whose crown is mainly below 27m. Therefore, these pixels have no meaning in terms of our  
397 LCA metric and do not represent large trees. This is why we chose to remove them. The goal of  
398 our study is to show that large trees are sufficient to estimate AGB. We clarified this point in the  
399 manuscript:

400 **Changes to manuscript:** ls.450-454: “Clusters smaller than 100 m<sup>2</sup> add only a small fraction  
401 (1.7% on average) to LCA values across sites. Including these clusters in LCA would not impact  
402 the performance of the model (similar  $R^2$ ,  $RMSE$  and  $bias$ ) and would allow to skip the final  
403 steps of the LCA retrieval (see Fig. S2). However, since these pixels either represent single  
404 branches reaching above 27m or the tip of a tree crown, they have no meaning in terms of our  
405 LCA metric and do not represent large trees.”.

406  
407 **Comment:** Technical comments: Inconsistent approach to using capitals in section headings.  
408 Line 209 – => Detecting changes of selective logging. Line 385 - => LCA as an AGB estimator  
409

410 **Response:** Thank you for pointing this out. We removed the capital letters accordingly.  
411

412

413

414

## 414 **Additional changes**

415 We made some additional minor edits to the paper to clarify some sentences. Please refer to the  
416 track changes of the revised manuscript, notably:

- 417 - Paragraph ls.485-503.
- 418 - Figure 6: “2012” was replaced by “2011”.
- 419 - The word “nine” was removed from the title to be more consistent with the content of the  
420 manuscript.

421

422

423

# Canopy Area of Large Trees Explains Aboveground Biomass Variations across Neotropical Forest Landscapes

Deleted: Nine

Victoria Meyer<sup>1,2</sup>, Sassan Saatchi<sup>1</sup>, David B. Clark<sup>3</sup>, Michael Keller<sup>4,5</sup>, Grégoire Vincent<sup>6</sup>, António Ferraz<sup>1</sup>, Fernando Espírito-Santo<sup>1,7</sup>, Marcus V.N. d'Oliveira<sup>5</sup>, Dahlia Kaki<sup>1</sup> and Jérôme Chave<sup>2</sup>

<sup>1</sup> Jet Propulsion Laboratory, California Institute of Technology, Pasadena, CA, USA

<sup>2</sup> Laboratoire Evolution et Diversité Biologique UMR 5174, CNRS Université Paul Sabatier, Toulouse, France

<sup>3</sup> Department of Biology, University of Missouri, St. Louis, Missouri, U.S.A.

<sup>4</sup> USDA Forest Service, International Institute of Tropical Forestry, San Juan, Puerto Rico

<sup>5</sup> EMBRAPA Acre, Rio Branco, Brazil

<sup>6</sup> IRD, UMR AMAP, Montpellier, 34000 France

<sup>7</sup> Lancaster Environmental Centre, Lancaster University, Lancaster, United Kingdom, LA1 4YQ

Correspondence to:

Victoria Meyer  
Jet Propulsion Laboratory  
California Institute of Technology  
4800 Oak Grove Drive  
Pasadena, CA. 91109 USA  
Email: victoria.meyer@jpl.nasa.com

37 **Abstract**

38 Large tropical trees store significant amounts of carbon in woody components and their  
39 distribution plays an important role in forest carbon stocks and dynamics. Here, we explore the  
40 properties of a new Lidar derived index, large tree canopy area (LCA) defined as the area  
41 occupied by canopy above a reference height. We hypothesize that this simple measure of forest  
42 structure representing the crown area of large canopy trees could consistently explain the  
43 landscape variations of forest volume and aboveground biomass (AGB) across a range of climate  
44 and edaphic conditions. To test this hypothesis, we assembled a unique dataset of high-resolution  
45 airborne Light Detection and Ranging (Lidar) and ground inventory data in nine undisturbed old  
46 growth Neotropical forests, [of which four had plots large enough \(1ha\) to calibrate our model](#).  
47 We found that the LCA for trees greater than 27 m (~25–30 m) in height and at least 100 m<sup>2</sup>  
48 crown size in a unit area (1 ha), explains more than 75 % of total forest volume variations,  
49 irrespective of the forest biogeographic conditions. When weighted by average wood density of  
50 the stand, LCA can be used as an unbiased estimator of AGB [across sites](#) ( $R^2 = 0.78$ , RMSE =  
51  $46.02 \text{ Mg ha}^{-1}$ , bias =  $-0.63 \text{ Mg ha}^{-1}$ ). Unlike other Lidar derived metrics with complex nonlinear  
52 relations to biomass, the relationship between LCA and AGB is linear [and remains unique across](#)  
53 [forest types](#). A comparison with tree inventories across the study sites indicates that LCA  
54 correlates best with the crown area (or basal area) of trees with diameter [greater than 50 cm](#). The  
55 spatial invariance of the LCA–AGB relationship across the Neotropics suggests a remarkable  
56 regularity of forest structure across the landscape and a new technique for systematic monitoring  
57 of large trees for their contribution to AGB and changes associated with selective logging, tree  
58 mortality, and other types of [tropical](#) forest disturbance and dynamics.

59

Deleted: 76

Deleted: . Results show that this

Deleted: relationship remains

Deleted: >

64 **Keywords**

65 Lidar, biomass, tropical forest, large trees, crown area, wood density

66

67 **1 Introduction**

68 In humid tropical forests, tree canopies contribute disproportionately to the exchange of water  
69 and carbon with the atmosphere through photosynthesis (Goldstein et al., 1998; Santiago et al.,  
70 2004). From a physical standpoint, canopies are rough interfaces formed by crowns of emergent  
71 and large trees, regularly disturbed by wind thrusts and gap dynamics. This structurally complex  
72 boundary layer is challenging for scaling of biogeochemical fluxes and modeling of vegetation  
73 dynamics (Baldocchi et al., 2003). Large canopy trees are among the first to be impacted by  
74 storms or heavy precipitation (Espírito-Santo et al., 2010), drought stress (Nepstad et al., 2007;  
75 Saatchi et al., 2013; Phillips et al., 2009), and fragmentation (Laurance et al., 2000), potentially  
76 leading to tree death and formation of large canopy gaps (Denslow, 1980; Espírito-Santo et al.,  
77 2014). Several studies suggest that forest canopies can show fractal properties that tend to evolve  
78 from a non-equilibrium state towards a self-organized critical state, involving gap formation and  
79 recovery (Pascual and Guichard, 2005; Solé and Manrubia, 1995), with crowns preferentially  
80 growing towards more sunlit parts of the canopy (Strigul et al., 2008).

81 Over the past decade, stand level canopy metrics have been increasingly derived using small  
82 footprint airborne Lidar systems (ALS), a widely used remote sensing technique to study the  
83 structure of forests (Kellner and Asner, 2009; Lefsky et al., 2002). Lidar derived mean [top](#)  
84 canopy height (MCH) is a good predictor of tropical forest aboveground carbon content and its  
85 spatial variability (Jubanski et al., 2013), but it does not provide information on the presence of  
86 large trees that are important when monitoring changes of forest biomass from logging and [other](#)

87 small scale disturbance (Bastin et al., 2015). Moreover, different forests with the same MCH  
88 may differ in their stem density, notably of large trees, and in stand mean wood density, two  
89 aspects that are important in constructing a robust model to infer AGB from lidar data (Asner et  
90 al., 2012; Mascaro et al., 2011). Ground observations suggest that stem density, basal area,  
91 height and crown size of large tropical trees may all be good indicators of forest AGB (Clark and  
92 Clark, 1996; Goodman et al., 2014). This implies that including information on crown area of  
93 individual large trees should improve carbon stock assessments, as confirmed in temperate and  
94 boreal regions (eg. Packalen et al., 2015; Popescu et al., 2003; Vauhkonen et al., 2011, 2014). In  
95 tropical forests, identifying and delineating crowns of large trees is a difficult and time  
96 consuming process due to the layered structure of the forest canopy and overlapping crowns  
97 (Zhou et al., 2010, but see Ferraz et al., 2016).

98 Here, we explore how the fractional area occupied by crowns of large trees in a forest stand can  
99 be used as a reliable indicator of forest biomass across a wide range of forest structure, climate  
100 and edaphic geographic variations. We define large tree canopy area (LCA) as a metric  
101 capturing the cluster of crowns of large trees within a forest patch using height and crown area  
102 measured by high resolution airborne Lidar measurements. Precisely, LCA is the number of  
103 pixels in the canopy height model above a reference height, and excluding the pixel clusters  
104 smaller than a reference area. Since this metric quantifies the proportional presence of large  
105 trees, it can be used to estimate AGB and monitor changes associated with the disturbance of  
106 large trees from mortality events and selective logging. We first explore the properties of LCA  
107 across a range of landscapes in the Neotropics. Next, we hypothesize that LCA is a good  
108 predictive metric of the spatial variations of AGB over a wide range of old growth forests.

109 To this end, we assembled a collection of airborne Lidar measurements and ground inventory  
110 data at nine sites in old growth Neotropical forests. The Lidar data provide variations in canopy  
111 height and distribution of large trees that allow us to address the following questions: 1) is there  
112 a single definition of LCA at the landscape scale across different sites? 2) does LCA metric  
113 capture variations of AGB?

Deleted: unique

114

## 115 **2 Materials and Methods**

### 116 **2.1 Study sites**

117 We studied the canopy structure at nine old growth lowland Neotropical forest sites that span a  
118 broad range of climatic and edaphic conditions (Fig. S1, Table 1). All sites are located in low  
119 elevation areas (less than 500 m above sea level) but have small scale surface topography that  
120 may influence the distribution of crown formations and gaps. These forests are for the most part  
121 undisturbed *terra firme* forests. Tapajós, Antimary and Cotriguaçu get the least rainfall, with  
122 approximately 2000mm yr<sup>-1</sup>, while La Selva and Chocó both receive more than 4000 mm yr<sup>-1</sup>  
123 (Table 1).

124 Permanent forest inventory plots were available for all sites except Cotriguaçu (Table 1). Sites  
125 where tree level inventory data were available were used to estimate the stand level aboveground  
126 biomass, thereafter referred to as AGB<sub>inv</sub>: BCI (50 plots of 1 ha each), Chocó (42 plots of 0.25 ha  
127 each), La Selva (11 plots of 1 ha each), Manaus (10 plots of 0.25 ha each), Nouragues (7 plots of  
128 1 ha each) and Tapajós (10 plots of 0.25 ha each). In these plots, all trees with a diameter at  
129 breast height (DBH) ≥10 cm have been mapped, measured and identified to the species. Trees  
130 with irregularities or buttresses were measured higher on the bole. Total tree height  
131 measurements were available for a subset of these trees. The method for calculating AGB<sub>inv</sub> from

133 forest inventories is reported in S.1 of the supplementary information. ~~Four sites (BCI, La Selva,~~  
 134 ~~Nouragues and Paracou) with 1 ha inventory plots, were used as “calibration sites” to compare~~  
 135 ~~the LCA metric and AGB. Sites with smaller plots were not used as calibration of LCA because~~  
 136 ~~of the probability of crowns of large trees extending outside the plot boundary and the~~  
 137 ~~introduction of uncertainty in estimating LCA from edge effects (Meyer et al., 2013; Packalen et~~  
 138 ~~al., 2015). For this reason, all plots smaller than 1 ha were excluded from the LCA analysis but~~  
 139 ~~were used in estimating average wood density for each site, which does not depend on plot size.~~  
 140 Stand averaged wood density was calculated based on the wood density of all trees present in a  
 141 site, determined using the commonly used global wood density database, and is reported in Table  
 142 1 (Chave et al., 2009; Zanne et al., 2009). For Cotriguaçu, we used stand averaged wood density  
 143 given by Fearnside, (1997) for a region covering the site. Additional plot level data (AGB<sub>inv</sub> and  
 144 mean wood density) were provided for Antimary (50 plots of 0.25 ha each), Nouragues (27 plots  
 145 of 1 ha each) and Paracou (85 plots of 1 ha each).

Moved (insertion) [1]

Deleted: were available were used

Deleted: , and are here referred to as “calibration sites” (BCI, La Selva, Nouragues and Paracou). Smaller plots have a higher probability of having the

Deleted: e

Deleted: , which can introduce

Deleted: because of edge effect

146  
 147

Moved up [1]: The four sites where 1 ha plots were available were used to compare the LCA metric and AGB, and are here referred to as “calibration sites” (BCI, La Selva, Nouragues and Paracou). Smaller plots have a higher probability of having the crown of large trees extend outside the plot boundary, which can introduce uncertainty in estimates of LCA because of edge effect (Meyer et al., 2013; Packalen et al., 2015). For this reason, all plots smaller than 1 ha were excluded from this analysis. .

## 148 2.2 Lidar data

149 Lidar sensors scan the vegetation vertical structure and return a three dimensional point cloud  
 150 derived from the time it took each pulse to return to the instrument. The Lidar datasets acquired  
 151 over the study sites come from discrete return Lidar instruments and were gridded horizontally at  
 152 a 1m resolution using the echoes classified as either vegetation or ground. They yield three  
 153 products: digital surface model (DSM) corresponding to the top canopy elevation, digital terrain  
 154 model (DTM) corresponding to the ground elevation, and canopy height model (CHM), which is  
 155 the height difference between the DSM and the DTM. DTMs were interpolated from a Delaunay



172 triangulation or comparable interpolation methods, after outliers have been removed. DSMs were  
173 created using the highest return within a cell. Lidar data over Paracou were acquired in last  
174 return mode, causing a bias of 50 cm on the CHM (Vincent et al., 2012). This bias is not  
175 addressed in this study because our height increment for the determination of optimal height  
176 thresholding is larger (1m) (see Sect. 4.3). Data were acquired between 2009 and 2013, using  
177 relatively similar sensors and acquisition configurations (Table 2). The potential differences  
178 between the Lidar datasets and their impact on the results are addressed in the Discussion.  
179 For each site, we selected a 1x1 km (100 ha) area of old growth forest, oriented north-south,  
180 without any human disturbance to the extent possible. Topography derived from Lidar data  
181 within the selected 1 km<sup>2</sup> subset images provides information on landscape variations that may  
182 impact the forest structure. Data visualization was done using ENVI version 4.8 (Exelis).

183

Deleted: - ... [1]

### 184 **2.3 Computing Large Canopy Area (LCA)**

185 At each study site, we extracted the area of canopy that relates to total area of the canopy height  
186 model above a standard height (h) threshold, or LCA(h), and explored how this metric scales  
187 along two axes. First, we varied the threshold height h with increments of 1m, between 5m and  
188 50m, in 100 m by 100 m subareas (100 subareas for each site). Second, to denoise the data, we  
189 excluded the clusters with less than a set number of 1m<sup>2</sup> pixels (50, 100, 150 or 200). We then  
190 prioritized the crown area of large trees, and filtered out pixels that could be related to outliers or  
191 to single branches. This method thus quantifies the area of large crowns covering a plot or larger  
192 landscape unit area, as a percentage of covered area.

193 LCA maps were produced at 1 ha resolution. Pixel clustering was based on the similarity of the  
194 four nearest neighbors (similar results were obtained with an eight\_neighbor model, results not

197 shown here). Figure S2 summarizes the steps taken to go from the Lidar canopy height model to  
198 the final LCA map. Processing was conducted using the IDL software (Interface Description  
199 Language, Exelis).

200 We determined the optimal minimum canopy height threshold calculating the coefficient of  
201 correlation between [AGB<sub>inv</sub> and LCA at the four calibration sites](#). This step allowed us to  
202 examine if optimal height thresholds differed from one site to the other. The goal was to find a  
203 single optimal height threshold and crown size that could be applied for LCA retrieval across  
204 closed canopy Neotropical forests. [We also estimated AGB from Lidar data locally \(AGB<sub>Local</sub>\)](#)  
205 [using a commonly used model fit relating MCH to AGB<sub>inv</sub> in each site, to further examine the](#)  
206 [variations of LCA and AGB in all nine sites \(see S.2, Table S1\)](#).

#### 208 2.4 Relating LCA to biomass

209 We tested different models to infer AGB<sub>inv</sub> from LCA, henceforth called AGB<sub>LCA</sub>, at the four  
210 calibration sites, and explored if adding more parameters, such as mean wood density of a site,  
211 mean wood density of large trees (DBH ≥50 cm), mean canopy height or top percentiles of  
212 canopy height improved the predicting power of the model. We evaluated our results by applying  
213 a jackknife validation to our regression models, based on 1000 iterations of bootstrapping. [The](#)  
214 [coefficients of correlation \(R<sup>2</sup>\), root mean square error \(RMSE\) and bias \(mean difference](#)  
215 [between the expected values of AGB and the observed values of AGB\) are reported for the](#)  
216 [models providing the best results.](#) The analysis was performed using the R statistical software (R  
217 Core Team, 2014).

218 [We compared the new approach based on LCA to a similar approach based on MCH, which](#)  
219 [relies on information on all pixels of an area of interest. In both cases, models were calibrated by](#)

**Deleted:** AGB<sub>Lidar</sub> and LCA

**Deleted:** We also performed the same analysis using AGB<sub>inv</sub> and LCA at the four calibration sites.

**Deleted:** Adding more parameters did not improve the performance of the model, except when using WD as a normalizing factor. The two models we retained are therefore of the form The two models we retained are of the form of Eq. (12) and Eq. (23): - ... [2]

**Deleted:** We also compared AGB as derived from LCA (AGB<sub>LCA</sub>) to the Lidar derived aboveground biomass (AGB<sub>Lidar</sub>) in the nine 1km<sup>2</sup> images. The coefficients of correlation (R<sup>2</sup>), root mean square error (RMSE) and bias (mean difference between the expected values of AGB and the observed values of AGB) are reported in Table 3. We finally compared these results to a traditional model relying on MCH to estimate AGB.

238 [using field data from the four calibration sites and their respective mean wood density. This](#)  
239 [comparison is meant to investigate if a metric based on large trees only \(LCA\) can estimate AGB](#)  
240 [similarly to a metric that uses information about 100% of the canopy \(MCH\).](#)

241

## 242 **2.5 Detecting changes of selecting logging**

243 Forest degradation due to selective logging is difficult to detect with conventional remote  
244 sensing techniques due to small scale and minor impacts on the forest canopy and biomass  
245 compared to severe forest disturbances (e.g. fires, storms, or clearing). However, selective  
246 logging targets large trees (Pearson et al., 2014) and thus may be detectable using LCA, [provided](#)  
247 [that lidar data are available from pre and post-logging](#). Here, we use the Antimary study site that  
248 was selectively logged after the 2010 Lidar acquisition to examine the use of LCA for detecting  
249 logging impacts on the forest canopy and AGB. We apply the large tree segmentation approach  
250 on both the 2010 [image](#) and on a 2011 post-logging Lidar [image](#) (see Andersen et al., 2014 for  
251 details) to quantify the logging impacts in terms of the distribution of large trees removed from  
252 the forest and the loss of aboveground biomass.

253

## 254 **3 Results**

### 255 **3.1 Intersite comparison of landscapes and MCH**

256 Topographic variation [within the 1 km<sup>2</sup> images](#) ranged from about 4 m elevation gain in flat area  
257 of Tapajós to steep elevation gain of up to about 100 m in Cotriguaçu and Chocó (Fig. S3). Top  
258 canopy height reached up to 60m, but varies across sites, with Chocó having the lowest MCH  
259 (24.1 m) and Nouragues the highest (29.7 m). Forest height in Manaus was more homogeneous  
260 than in the other sites, with a standard deviation of 6.8 m for MCH, versus 10.3 m in Paracou.

Deleted: S

Deleted: C

Deleted: S

Deleted: L

Deleted: data

266 We found no relationship between topography and canopy height, which suggests that variability  
267 in forest structure may be due to other ecological and edaphic factors in each site.

268  
269

### 270 **3.2 Large canopy area index**

271 The choice of the canopy height threshold impacted LCA more than the minimum number of  
272 pixels per cluster (Table S2). The difference due to the choice of the minimal cluster size  
273 threshold was on average 1.4 %, calculated as the mean of the difference between the smallest  
274 grain (50 pixels) and the largest one (200 pixels) across sites and height thresholds. Based on this  
275 analysis, we chose to define LCA using a minimum cluster size of 100 pixels (100 m<sup>2</sup> for crown  
276 area) in the remainder of this study. This corresponds to an area of at least 10 m x10 m or a circle  
277 of approximately 11 m in diameter, consistent with the average crown diameter of large trees of  
278 the region (Bohlman and O'Brien, 2006; Figueiredo et al., 2016; Clark, unpublished results).

279

280 In contrast, the canopy height thresholds markedly impacted the magnitude of LCA among sites  
281 (Fig. 1 and Fig. 2, Table S2). As the height threshold increased, intra-site variation of LCA(h)  
282 became apparent, showing differences of LCA associated with differences of forest structure  
283 (Fig. 1). Tapajós and Nouragues stood out with more area of large trees at the height threshold of  
284 30 m ( $LCA_{30m} = 51$  and 48 %, respectively) , while Antimary and Chocó showed much lower  
285 LCA at this height threshold ( $LCA_{30m} = 21$  %) (Table S2). The steepest slopes of the LCA(h)  
286 function corresponded to the highest sensitivity of LCA to height thresholds and the inflection in  
287 LCA was found between 24m in Antimary and 30m in Nouragues (Fig. 2). The average height  
288 of the steepest slope was about 27 m, a value that was used as the optimal threshold across all  
289 sites.

290 [Regressing](#)  $AGB_{inv}$  and LCA at the calibration sites (Fig. 3b) [showed](#) the best relationships  
 291 corresponded to height thresholds [between 27m \(Nouragues and Paracou\) and 28m \(BCI and La](#)  
 292 [Selva\)](#), with maximum coefficients of correlation ranging between 0.5 and 0.8. [The same](#)  
 293 [analysis repeated using  \$AGB\_{local}\$  and LCA in the nine sites also confirmed the earlier results that](#)  
 294 [the highest coefficients of correlation between the two metrics occurred between 23 m \(Chocó\)](#)  
 295 [and 30 m \(Tapajós\) height thresholds \(Fig. 3a\), explaining more than 75 % of AGB variation in](#)  
 296 [each site](#). Based on these results, we defined LCA as the cumulative area of clusters of the  
 297 canopy height model greater than 27 m height, [as the mean of optimal height threshold with](#)  
 298 [highest  \$R^2\$  across sites, with clusters covering areas larger than 100 m<sup>2</sup>](#).

**Deleted:** Regressing  $AGB_{Lidar}$  and LCA showed that the highest coefficients of correlation between the two metrics occurred between 23 m (Chocó) and 30 m (Tapajós) height thresholds (Fig. 3a), explaining more than 75 % of AGB variation in each site. The same analysis repeated using

**Deleted:** also confirmed the earlier results

**Deleted:** ing

**Deleted:** are found to be

### 300 3.3 Variation of AGB derived from LCA

302  $AGB_{inv}$  was found to depend linearly on LCA (Eq. 1), with a better coefficient of correlation and  
 303 RMSE than a power law fit ( $R^2_{linear} = 0.59$ ,  $RMSE_{linear} = 62.53 \text{ Mg ha}^{-1}$ , vs.  $R^2_{power} = 0.54$ ,  
 304  $RMSE_{power} = 65.38$ ). Although this model was unbiased ( $bias_{cross\_val} = 0.16 \text{ Mg}$ ), there were clear  
 305 differences among study sites (Fig. 4a, Table 3). These differences were largely explained by  
 306 landscape scale differences in wood density, an important factor representing the influence of  
 307 species composition on the spatial variation of AGB. [Since AGB depends on DBH, H and WD](#)  
 308 [\(see Chave et al., 2014\), average wood volume can be computed approximately as the ratio of](#)  
 309 AGB divided by the average wood density (Fig. 4b). The linear relationship between LCA and  
 310 wood volume yielded an estimate of the average total volume of forests independently of the site  
 311 characteristics, through  $Vol = a LCA + b$ . [Adding more parameters did not improve the](#)

**Deleted:** 2

**Deleted:** other models, such as

**Deleted:** bias = 0.0 Mg,

**Deleted:** 05

**Deleted:** To explore the contribution of wood density across the study sites,

**Deleted:** we

**Deleted:** the average wood volume

**Deleted:** as

**Deleted:** (Table 3)

330 [performance of the model, except when using WD as a normalizing factor. The two models we](#)  
 331 [retained are therefore of the form of Eq. \(1\) and Eq. \(2\):](#)

332  $AGB_{LCA} = a LCA + b$  (1)

333  $AGB_{LCA} = (a LCA + b) \times WD$  (2)

334 where here WD is the mean wood density of a site. The coefficients of the models, as well as  
 335 their respective coefficients of correlation, RMSE and bias [from training data and cross-](#)  
 336 [validation](#) are reported in Table 3.

337 For AGB estimation, the model based on LCA weighted by WD gives the best result by bringing  
 338  $R^2$  up to 0.78 and RMSE down to 46.02 Mg ha<sup>-1</sup> (Fig. 4b, Fig. [4c](#), Table 3, Eq. (2)), with  $AGB_{inv}$   
 339 and  $AGB_{LCA}$  falling around a one-to-one line in Fig. [4c](#). At all sites, RMSE values are between  
 340 20.87 and 42.22 Mg, except Nouragues, where RMSE remains large (71.21 Mg) due to high  
 341 biomass and several outliers from the linear relation. [The relationship between LCA and other](#)  
 342 [metrics derived from ground data, such as Lorey's height or basal area, are presented in S.3 and](#)  
 343 [Table S4.](#)

344  
 345 **[3.4 LCA vs. MCH approach](#)**

346 [Finally, we compared these results to AGB estimated using a similar approach based on MCH](#)  
 347 [\( \$AGB\_{MCH}\$ \) for the calibration plots \(Fig. 5a\), and we also compared  \$AGB\_{LCA}\$  to  \$AGB\_{MCH}\$  in all](#)  
 348 [nine sites, using LCA and MCH of the 1km<sup>2</sup> images \(Fig. 5b\).](#)  
 349 [Both methods perform similarly \( \$R^2\_{MCH} = 0.80\$ ,  \$RMSE\_{MCH} = 42.52\$  Mg ha<sup>-1</sup>,  \$bias\_{cross\ val} = -0.21\$  Mg](#)  
 350 [ha<sup>-1</sup>, Table S3\), showing that relying on a fraction of the Lidar information performs as well as](#)  
 351 [using a metric depending on information from all pixels. However, Fig. 5 also shows that the](#)

Deleted: ,

Deleted: 5

Deleted: 3

Deleted: 5a

Deleted:

Deleted: b

Deleted: ,

Deleted: applied the model from Eq. (3) to all 1km<sup>2</sup> areas and

Deleted: the derived

Deleted: AGBLidar

Deleted: (see Sect. 2.2)

Deleted: , for which local models based on MCH were used

Deleted: cb

Deleted: . Global RMSE was found to be 34.72 Mg and RMSE per site varied between 20.79 Mg at BCI and 49.58 Mg at Manaus

Deleted: Our ground calibrated LCA model defined by Eq. (3) had a similar performance as the MCH based AGB model ( $R^2_{MCH} = 0.79$ ,  $RMSE_{MCH} = 44.2$  Mg, Table S3). These findings

Deleted: gives comparable results

Deleted: s

Deleted: , such as MCH

Deleted: ure 5b and 5c

378 [LCA method tends to overestimate AGB compared to the MCH method \(bias=9.66 Mg ha<sup>-1</sup>\),](#)  
379 [especially in La Selva, BCI, Cotriguaçu and Manaus.](#)

Deleted: , highlighting the importance of large canopy trees to estimate biomass. The relationship between LCA and other metrics derived from ground data, such as Lorey's height or basal area, are presented in Table S4.

### 381 **3.5 AGB changes from logging**

Deleted: 4

382 The impacts of logging on the distribution of large trees and changes of AGB was detected by  
383 simply deriving the LCA index from pre and post-logging Lidar data acquired in 2010 and 2011  
384 respectively in Antimary (Fig. 6). Difference in LCA between the two dates (2010–2011) (Fig.  
385 6a) at 1 ha grid cell captured the areas of largest changes in the few months following logging  
386 (logging took place between June and November 2011, Lidar data were collected in late  
387 November 2011). The LCA approach was able to detect approximately a 17 % decrease in LCA,  
388 from a mean LCA of 34.8 % in 2010 to 29.2 % in 2011.

389 The changes were also captured in the frequency distribution of large canopy trees before and  
390 after logging (Fig. 6b) and the differences in the spatial distribution (Fig. 6c and 6d).

391 These changes in LCA correspond to a biomass loss of 15.2 Mg ha<sup>-1</sup> when integrated in equation

392 [\(2\)](#) and were of the same magnitude of the planned selectively logging removal rate (12–18 Mg

Deleted: 2

393 ha<sup>-1</sup> or 10–15 m<sup>3</sup> ha<sup>-1</sup> of timber volume) (Andersen et al., 2014). [As a comparison, the MCH](#)

Deleted: 3

394 [model led to an estimated biomass loss of 19 Mg ha<sup>-1</sup>.](#) Difference in the Lidar index ( $\Delta LCA$ ) at

395 the native resolution of 1 m (Fig. 6e) was able to capture both the location of all large trees

396 removed from the forest stand and partial regeneration and gap filling that occurred in the forest  
397 between the two dates.

398

## 399 **4 Discussion**

### 400 **4.1 Inter-site Comparisons**

408 Cross-site studies on the structure of tropical forests have led to significant advances in our  
409 understanding of tropical forest ecology (Gentry 1993; Phillips et al., 1998; ter Steege et al.,  
410 2006). They have also yielded important insights on new techniques to predict carbon stocks  
411 across regions (eg. Asner and Mascaro, 2014). Comparison of sites in terms of MCH derived  
412 for the study sites confirms that there is a strong regional variation of AGB with respect to  
413 canopy height, and that East Amazonian sites tend to have much taller trees than Central and  
414 Western Amazonia sites. This was already apparent in the canopy height maps produced by the  
415 GLAS sensor (Lefsky, 2010; Saatchi et al., 2011; Simard et al., 2011). Comparing sites in terms  
416 of LCA showed a similar pattern of larger trees, being relatively more present in eastern  
417 Amazonia, notably in the French Guiana sites and Tapajos. Our most southwestern site was  
418 Antimary, in the state of Acre (Brazilian Amazon). ~~However, this site does not represent forests~~  
419 ~~in the western Amazon or the Amazon-Andes gradients with relatively lower wood density~~  
420 ~~(Baker et al. 2004) and more fertile volcanic soils impacting the forest structure and dynamics~~  
421 ~~(Quesada et al., 2011).~~ The site in Chocó is also unique in its characteristics because of  
422 extremely wet condition and ~~potential disturbance~~ (e.g., selective logging). Additional lidar and  
423 ground measurements ~~will allow validating the performance of the LCA in representing the AGB~~  
424 ~~variations in the western Amazon region.~~

Deleted: areas in

Deleted:

Deleted: the Peruvian Amazon and western

Deleted: unknown

Deleted: history

Deleted: would be needed in western Amazonia

Deleted: to further

Deleted: the patterns observed in this study.

#### 426 4.2 Physical Interpretation of LCA

427 In this study, we introduced a simple structural metric that captures the proportion of area  
428 covered by large trees over the landscape (> 1 ha) and explained 78% of the variation in average  
429 forest volume and biomass when weighted by wood density in ~~four~~ sites of old growth  
430 Neotropical forests. LCA cannot separate the crown areas of individual trees. However, it is

Deleted: nine



440 adapted for large scale monitoring of forest volume and biomass change, as it is a robust and  
441 readily accessible metric. For individual tree separation, complex and more computationally  
442 intensive approaches are available (Ferraz et al., 2016).

443 In estimating LCA from Lidar data, we examined the spatial clustering properties of LCA and  
444 found that the minimum cluster size was less important than the threshold of canopy height, as  
445 long as the analysis focused on the relative covered area instead of on the density of large trees.  
446 We found that using the percentage of the area covered by large canopy trees is an efficient way  
447 of overcoming the problem of individual crown segmentation in Lidar data. LCA is related to  
448 how trees reaching the forest canopy (above a certain height) fill the space and how this  
449 characteristic may follow a spatially invariant scaling across tropical forests (West et al., 2009).

450 [Clusters smaller than 100 m<sup>2</sup> add only a small fraction \(1.7% on average\) to LCA values across](#)  
451 [sites. Including these clusters in LCA would not impact the performance of the model \(similar](#)  
452 [R<sup>2</sup>, RMSE and bias\) and would allow to skip the final steps of the LCA retrieval \(see Fig. S2\).](#)  
453 [However, since these pixels either represent single branches reaching above 27m or the tip of a](#)  
454 [tree crown, they have no meaning in terms of our LCA metric and do not represent large trees.](#)  
455 [LCA provides information on the presence of large trees in a study area, which other metrics](#)  
456 [such as MCH cannot do. It is an important point, considering that large trees are often the most](#)  
457 [affected by natural disturbance and targeted by logging companies.](#)

458

### 459 **4.3 Correlation between LCA and AGB**

460 The distribution of R<sup>2</sup> between LCA and AGB for (Fig. 3) is such that the maximum difference in  
461 R<sup>2</sup> between a threshold of 25m and 30m is approximately 0.1, a negligible value. Hence, AGB  
462 retrieval by LCA is relatively insensitive to the height threshold. For most sites, except

463 Antimarily, we found a height threshold such that LCA explains about 80–90 % of the variation of  
464 AGB or total volume of the forests for each site (60–70 % when compared with ground plots)  
465 (Fig. 3). Using a height threshold of 27 m for all sites reduced the  $R^2$  by 0.04 on average (max =  
466 0.08) compared to the optimal height threshold for each site.  
467 Potential differences in MCH among sites are due to footprint size, scan angle and return density  
468 (Disney et al., 2010; Hirata, 2004; Hopkinson, 2007) (Table 2). However, these effects are  
469 generally smaller than the 1m increment that we used to determine the optimal height thresholds  
470 of LCA. As a result, LCA estimation, and therefore AGB inferred from LCA, should depend  
471 little on instrument, acquisition and processing (Table 2). This is an important finding given the  
472 increasing variety of airborne Lidar sensors, and also given the pre and post-processing methods  
473 available for monitoring tropical forest structure and aboveground biomass. However,  
474 determining whether the 27m threshold holds for LCA calculation across in the tropics would  
475 require a validation at more study studies across continents.

**Deleted:** Hence, the difference between the  $R^2$  of Lidar and ground plots is due to the relative correlation between MCH used in Lidar derived biomass and LCA. Differences in Lidar characteristics for each site and differences in timing of Lidar observations and ground plots further amplify this problem. Finally, a limit to how much LCA can explain variation in AGB relates to forest structure and the AGB of small trees.

#### 477 4.4 LCA Relation to Ground Measurements

478 The relation between LCA derived from Lidar and the ground measurements can be further  
479 investigated by converting the 27 m height threshold into equivalent DBH values, using a  
480 height–diameter relationship. In the absence of a local DBH–height relation at each site, we  
481 made use of the following equation (Chave et al., 2014):

$$482 \quad \ln(H) = 0.893 - E + 0.760 \times \ln(D) - 0.0340 \times (\ln(D))^2 \quad (3)$$

483 where E is a measure of environmental stress for each site that potentially impacts the tree  
484 allometry. The corresponding DBH values fall around 35–55 cm, except for Chocó, where the  
485 best coefficient of correlation is reached with a DBH threshold of 29 cm (Fig. S4). The average

**Deleted:** Our ground calibrated LCA model defined by Eq. (3) had a similar performance as the MCH based AGB model ( $R^2_{MCH} = 0.79$ ,  $RMSE_{MCH} = 44.2$  Mg, Table S3).

**Deleted:** 4

498 minimum DBH to assign for the definition of large trees that represent variations of AGB is  
499 below 50 cm. By choosing a DBH threshold of 50 cm for old-growth undisturbed forests, the  
500 LCA model for estimating biomass can have an approximate analog in inventory data. This  
501 comparison suggests that the LCA model can also be adjusted with the average wood density of  
502 trees larger than 50 m, allowing a much faster ground data collection of calibrating LCA model  
503 for different sites (S.4). ↓  
504 A limit to how much LCA can explain variations in AGB relates to forest structure and the AGB  
505 of small trees. The lower range of biomass estimation for the LCA model, associated with the  
506 intercept for LCA equal to zero, ranged between 122 Mg ha<sup>-1</sup> in La Selva and 192 Mg ha<sup>-1</sup> in  
507 Paracou (Fig. 7a). This lower range identified with the intercept of the LCA–AGB linear model  
508 can be interpreted as the AGB associated with all trees smaller than 27 m height (approximately  
509 all trees with DBH <50 cm). Note that the differences between sites are due to differences in  
510 their mean wood density and not the volume of trees (see Eq. (2) and Fig. 4). Similarly, the  
511 contribution of small trees to the total biomass in the ground inventory ranges between around  
512 100 and 200 Mg ha<sup>-1</sup>, except in Paracou (261 Mg ha<sup>-1</sup>) (Fig. 7b). AGB estimation based on LCA  
513 in these sites cannot go under 100 Mg ha<sup>-1</sup> or over 500 Mg ha<sup>-1</sup>. This is not a limitation of the  
514 model because LCA is designed to provide AGB estimates for forests reaching at least 27 m in  
515 mean canopy height, and such forests generally exceed 100 Mg ha<sup>-1</sup> in AGB. Also, the upper  
516 threshold of 500 Mg ha<sup>-1</sup> is consistent with upper values found globally at 1 ha scale (Brienen et  
517 al., 2015; Slik et al., 2013). A recalibration of the method should be envisaged in secondary and  
518 highly degraded forests.

519  
520

**Deleted:** DBH estimation suggests that using a minimal DBH threshold of about 50 cm for large trees for old growth neo-tropical forests better represents the total AGB variations.

**Deleted:** Finally, a

**Deleted:** of

**Deleted:**

**Deleted:** only

**Deleted:** 3

530 **4.5 LCA as AGB Estimator**

531 The correlation of LCA to  $AGB_{inv}$  suggests that a Lidar based approach can lead to the  
532 estimation of AGB at the landscape scale and give useful information on the presence of large  
533 canopy trees and their distribution, extending the analysis of large trees in plot level inventory  
534 based studies (Bastin et al., 2015; Slik et al., 2013).

535 Therefore, LCA can explain the variations of total forest volume without any ancillary data about  
536 the forest or the landscape. Most bias in conversion of LCA to AGB, however, can be corrected

Deleted: Any

537 across landscapes and sites by scaling the LCA–AGB relationship with average wood density at  
538 the landscape scale. Our model can therefore potentially be applied to a wide range of forest  
539 types, provided that there is information about wood density of the study area in the literature.

540 Wood density has been shown to be a key element of allometric models of AGB estimation  
541 (Baker et al., 2004; Brown et al., 1989; Chave et al., 2004; Nogueira et al., 2007). If wood  
542 density is assumed to be constant across DBH classes, the mean wood density at the plot scale  
543 can readily be used to scale LCA to biomass. However, if the wood density of large trees is  
544 smaller or larger than the average wood density, (e.g. in BCI and Chocó: S.4, Fig. S5), the use of

Deleted: 3

545 mean wood density to scale LCA may introduce a slight bias in biomass estimation. A difference  
546 in mean wood density of  $0.1 \text{ g cm}^{-3}$  would introduce a bias of  $\pm 10\%$  in the biomass estimation  
547 when using our model. We found that using mean wood density of large trees or basal area  
548 weighted wood density instead can give slightly better results and could circumvent the

549 differences in size distribution of the wood density (S.4). Instead we could rely on the wood  
550 density of large trees only. This would make the collection of ground data easier and cost  
551 effective for biomass estimation, because trees  $\geq 50$  cm DBH only represent 5–10 % of the stems

Deleted: 3

552 of a plot (S.4, Fig. S6). Focusing on the wood density of dominant or hyper dominant species

Deleted: 3

557 could also be an alternative approach for future use of Lidar derived LCA for large scale biomass  
558 estimation (Fauset et al., 2015; ter Steege et al., 2013). [In the absence of information on wood](#)  
559 [density from the literature, modelled wood density could potentially be used, but would give](#)  
560 [greater errors. These errors should be taken into account when reporting on the uncertainty of the](#)  
561 [results.](#)

#### 563 [4.6 LCA and MCH](#)

564 [The comparison of LCA and MCH metrics showed that both performed similarly in estimating](#)  
565 [AGB, highlighting the importance of large canopy trees to estimate biomass. The differences](#)  
566 [between the two methods in estimating AGB show that two methods can have similar](#)  
567 [performance in terms of R<sup>2</sup> and RMSE and nonetheless lead to different estimations, with LCA](#)  
568 [giving higher AGB estimations in some sites. The choice of a metric is therefore crucial to](#)  
569 [estimate AGB, especially when estimating the changes in biomass \(see Section 4.7\).](#)

570 Both MCH and LCA–AGB models performed relatively poorly in high biomass plots of the  
571 Nouragues study area, by underestimating biomass values [greater than 500 Mg ha<sup>-1</sup>](#) (Fig. 4 and  
572 5). To explain the underestimation, we performed three tests: 1. We examined the differences in  
573 the ground estimated biomass values with and without tree height and found no significant  
574 impact in reducing the effect of underestimation. 2. We tested the hypothesis that the height  
575 threshold used for LCA estimation across sites was not suitable for the Nouragues study site and  
576 dismissed the hypothesis because 27 m was found to be the optimum threshold for Nouragues  
577 plots. 3. We examined the errors in the Lidar estimation of forest height and found that except  
578 for an extremely high AGB<sub>inv</sub> of 617 Mg ha<sup>-1</sup>, the four other high biomass outliers are all located  
579 in the 6 ha Pararé plot located on a very steep topography. The Lidar digital terrain model

Deleted: models

Deleted: 6

Deleted:

Deleted:

584 (DTM) of this area shows an average within plots elevation range of 90 m. Ground detection on  
585 steep terrain can be erroneous, depending on the Lidar point density and the view angle, causing  
586 large area interpolation errors for DTM development and significant error in canopy height  
587 measurements (Leitold et al., 2015). Other factors that may affect the underestimation of AGB  
588 by LCA or MCH in the Nouragues site may be due to the presence of forest patches with clusters  
589 of large trees and overlapping crown areas. [It is also possible that the relationship between AGB  
590 and LCA is not linear for very high AGB values. This could be tested in the future with a larger  
591 number of sites with very high biomass.](#)

#### 593 **4.7. LCA and forest degradation**

594 Although LCA and MCH may perform similarly in capturing the forest biomass variations and  
595 changes, the use of LCA in detecting forest degradation and logging is more straightforward  
596 because of its relation to large trees. The LCA approach was able to accurately detect changes  
597 in forests after logging by locating where the large trees are extracted. Our estimate of biomass  
598 change from the LCA approach was higher than the biomass loss of 9.1 Mg ha<sup>-1</sup> reported by  
599 another study using the 25<sup>th</sup> percentile height above ground as the Lidar metric for biomass  
600 estimation (Andersen et al. 2014). It can be expected that relying on the 25<sup>th</sup> percentile height  
601 metric for biomass estimation would place more emphasis on the lower part of the canopy  
602 (understory) that is either less damaged or has gone through some level of regeneration after  
603 logging. Models based on LCA or MCH, on the other hand, may be more realistic for estimating  
604 AGB changes because they capture the changes in large trees and upper forest canopy structure  
605 that contain most of the biomass and are directly impacted by logging and biomass removal.

Deleted: 6

607 [The higher biomass loss estimation from the MCH model \(19 Mg ha<sup>-1</sup>\) again shows how](#)  
608 [different metrics can lead to different results. Here, three methods based on three different Lidar](#)  
609 [metrics yielded results that differed by more than twofold. LCA could become an important tool](#)  
610 [to detect forest degradation, in particular selective logging, considering that large trees are](#)  
611 [targeted by logging companies.](#)

612

#### 613 **4.8. Future Applications of LCA**

614 LCA definition in our study relies on the high resolution information on forest height, allowing  
615 for the detection of crown area of large canopy trees. Can a similar measure be derived from  
616 large footprint Lidar observations such as the future NASA spaceborne Lidar mission GEDI  
617 (Global Ecosystem Dynamic Investigation)? GEDI will not provide spatially continuous data  
618 on forest height, but its footprint size (~ 25 m) and dense sampling may be adequate to develop  
619 statistical indicators of large trees over the landscape.

620 Similarly, future spaceborne radar missions could also provide useful information to retrieve  
621 large canopy areas. The synthetic aperture radar (SAR) tomographical observations of the  
622 European Space Agency (ESA) BIOMASS mission will provide wall-to-wall imagery of canopy  
623 profile that could be converted to LCA over the landscape (Le Toan et al., 2011). Preliminary  
624 research based on airborne TomoSAR measurements has already shown that backscatter power  
625 at about 30 m above the ground, with sensitivity to the distribution of large trees, explained the  
626 variation of AGB over Nouragues and Paracou plots better than the backscatter power related to  
627 the lower part of the canopy (0–15 m) (Minh et al., 2016; Rocca et al., 2014). Future research on  
628 exploring the use of an equivalent radar index product from BIOMASS height or tomography

Deleted: 7

630 measurements at a height threshold (e.g. 27 m) may provide a potential algorithm to map the area  
631 of large trees and estimate forest volume and biomass changes across the landscape.

632

633

## 634 **5 Conclusions**

635 We introduce LCA as a new Lidar derived index to capture the variations of large trees and total  
636 volume and biomass across landscapes that remain spatially and regionally invariant. The  
637 importance of LCA is in its relevance to the structure and ecological characteristics of large trees  
638 in filling the canopy space and their unique contribution in determining the total volume and  
639 biomass of forests. Unlike other Lidar derived metrics, LCA is linearly related to total

640 aboveground biomass after being weighted by average wood density. [This linear relationship](#)

641 [remains unique across different forest types, making the LCA model broadly applicable.](#) The

642 comparison of LCA index with ground plots suggests that DBH >50 cm is a more reliable

643 threshold to quantify the number and distribution of large trees [in undisturbed old growth](#)

644 [tropical forests](#) and in capturing the variations of the total aboveground biomass across

645 landscapes and regions. [The results of our study may encourage further research in the use of](#)

646 [Lidar data for detecting the distribution of larger trees in tropical forests for ecological and](#)

647 [conservation studies.](#)

648

649

## 650 **Author contribution**

651 V. Meyer and S. Saatchi developed the model and designed the study. V. Meyer developed the

652 model code and performed the analysis. J. Chave, G. Vincent, M. Keller, F. Espirito-Santo, D.



653 Clark and M. d'Oliveira provided inventory data and derived metrics necessary to run the  
654 experiments. A. Ferraz contributed to the data processing. D. Kaki performed a preliminary  
655 analysis of the data. V. Meyer prepared the manuscript with contributions from all co-authors.  
656 The authors declare that they have no conflict of interest.

657

## 658 **Acknowledgements**

659 The work described in this paper was carried out at the Jet Propulsion Laboratory, California  
660 Institute of Technology, under contract with the National Aeronautics and Space Administration.  
661 This work has benefited from “*Investissement d’Avenir*” grants managed by the French *Agence*  
662 *Nationale de la Recherche* (CEBA, ref. ANR-10-LABX-25-01 and TULIP, ref. ANR-10-LABX-  
663 0041; ANAEE-France: ANR-11-INBS-0001) and from CNES (TOSCA project; PI T Le Toan).  
664 Field and Lidar data from the Brazilian sites were acquired by the Sustainable Landscapes Brazil  
665 project supported by the Brazilian Agricultural Research Corporation (EMBRAPA), the US  
666 Forest Service, and USAID, and the US Department of State. La Selva field work was supported  
667 by the U.S. National Science Foundation LTREB Program NSF LTREB 1357177. Data in Chocó  
668 are available as part of the Reducing Emissions from Deforestation and forest Degradation  
669 (REDD) project. FES was supported by Natural Environment Research Council (NERC) grants  
670 (‘BIO-RED’ NE/N012542/1 and ‘AFIRE’ NE/P004512/1) and Newton Fund (‘The UK  
671 Academies/FAPESP Proc. N<sup>o</sup>: 2015/50392-8 Fellowship and Research Mobility’). The AGB  
672 data for Paracou were made available courtesy of CIRAD (B. Hérault).

673  
674 © 2017. All rights reserved.

675  
676  
677

## 678 **Data accessibility**

679 The BCI lidar and forest inventory dataset used in this research are publically available from the  
680 Office of Bioinformatics, Smithsonian Tropical Research Institute. All relevant data are within  
681 the paper and its Supporting Information files.

682

683

## 684 **References**

685

686 Andersen, H. E., Reutebuch, S. E., McGaughey, R. J., d'Oliveira, M. V. and Keller, M.:  
687 Monitoring selective logging in western Amazonia with repeat lidar flights. *Remote Sens.*  
688 *Environ.*, 151, 157-165, 2014.

|

689  
690 Asner, G. P., Mascaro, J., Muller-Landau, H. C., Vieilledent, G., Vaudry, R., Rasamoelina, M.,  
691 Hall, J. S. and van Breugel, M.: A universal airborne Lidar approach for tropical forest carbon  
692 mapping. *Oecologia*, 168(4), 1147-1160, 2012.  
693  
694 Asner, G. P. and Mascaro, J.: Mapping tropical forest carbon: Calibrating plot estimates to a simple  
695 Lidar metric. *Remote Sens. Environ.* 140, 614-624, 2014.  
696  
697 Baker, T. R., Phillips, O. L., Malhi, Y., Almeida, S., Arroyo, L., Di Fiore, A., Erwin, T., Killeen,  
698 T. J., Laurance, S. G., Laurance, W. F. and Lewis, S. L.: Variation in wood density determines  
699 spatial patterns in Amazonian forest biomass. *Glob. Change Biol.*, 10(5), 545-562. doi:  
700 10.1111/j.1365-2486.2004.00751.x, 2004.  
701  
702 Baldocchi, D. D.: Assessing the eddy covariance technique for evaluating carbon dioxide exchange  
703 rates of ecosystems: past, present and future. *Glob. Change Biol.*, 9(4), 479-492, 2003.  
704  
705 Basset, Y., Cizek, L., Cuénoud, P., Didham, R. K., Guilhaumon, F., Missa, O., Novotny, V.,  
706 Ødegaard, F., Roslin, T., Schmid, J. and Tishechkin, A. K.: Arthropod diversity in a tropical  
707 forest. *Science*, 338(6113), 1481-1484, 2012.  
708  
709 Bastin, J.-F., Barbier, N., Réjou-Méchain, M., Fayolle, A., Gourlet-Fleury, S., Maniatis, D., de  
710 Haulleville, T., Baya, F., Beeckman, H., Beina, D. and Couteron, P.: Seeing Central African forests  
711 through their largest trees. *Sci. Rep.-UK*, 5, 13156, 2015.  
712  
713 [Bioredd.org/](http://Bioredd.org/) accessed 4.13.2016  
714  
715 Bohlman, S., and O'Brien, S.: Allometry, adult stature and regeneration requirement of 65 tree  
716 species on Barro Colorado Island, Panama. *J. Trop. Ecol.*, 22(02), 123-136, 2006.  
717  
718 Brienen, R. J. W., Phillips, O. L., Feldpausch T. R., Gloor E., Baker, T. R., Lloyd, J. and Lopez-  
719 Gonzalez G.: Long-Term Decline of the Amazon Carbon Sink. *Nature*, 519, 344.  
720 <http://dx.doi.org/10.1038/nature14283>, 2015.  
721  
722 Brown, S., Gillespie, A. J., and Lugo, A. E.: Biomass estimation methods for tropical forests with  
723 applications to forest inventory data. *Forest Sci.*, 35(4), 881-902, 1989.  
724  
725 Chave, J., Condit, R., Aguilar, S., Hernandez, A., Lao, S., and Perez, R.: Error propagation and  
726 scaling for tropical forest biomass estimates, *Philos. T. R. Soc. B*, 359, 409-420, 2004.  
727  
728 Chave, J., Réjou-Méchain, M., Búrquez, A., Chidumayo, E., Colgan, M. S., Delitti, W. B., and  
729 Vieilledent, G.: Improved allometric models to estimate the aboveground biomass of tropical trees.  
730 *Glob. Change Biol.*, 20(10), 3177-3190, 2014.  
731  
732 Clark D. B. and Clark D. A.: Abundance, growth and mortality of very large trees in neotropical  
733 lowland rain forest. *Forest Ecol. and Manag.*, 80, 235-244, 1996.  
734

735 Clark, D. B. and Clark, D. A.: Landscape-scale variation in forest structure and biomass in a  
736 tropical rain forest. *Forest Ecol. and Manag.*, 137, 185–198, 2000.  
737  
738 Condit, R.: *Tropical Forest Census Plots*. Springer Verlag and R.G. Landes Company. Berlin and  
739 Georgetown, TX, 1998.  
740  
741 d'Oliveira, M. V. N., Reutebuch, S. E., McGaughey, R. J. and Andersen, H. E. : Estimating  
742 forest biomass and identifying low-intensity logging areas using airborne scanning lidar in  
743 Antimary State Forest, Acre State, Western Brazilian Amazon. *Remote Sens. Environ.*, 124, 479-  
744 491, 2012.  
745  
746 Denslow, J. S. : Gap portioning among tropical rainforest trees. *Biotropica*, 12, 47–55, 1980.  
747  
748 Disney, M. I., Kalogirou, V., Lewis, P., Prieto-Blanco, A., Hancock, S., and Pfeifer, M.:  
749 Simulating the impact of discrete-return Lidar system and survey characteristics over young  
750 conifer and broadleaf forests. *Remote Sens. Environ.*, 114(7), 1546-1560, 2010.  
751  
752 ENVI/IDL, Exelis Visual Information Solutions, Boulder, Colorado.  
753  
754 Espirito-Santo, F. D. B., Keller, M., Braswell, B., Nelson, B. W., Froking, S., and Vicente, G.:  
755 Storm intensity and old-growth forest disturbances in the Amazon region. *Geophys. Res. Lett.*,  
756 37(11), 2010.  
757  
758 Espirito-Santo, F. D. B., Keller, M. M., Linder, E., Oliveira, R. C. Junior, Pereira, C. and  
759 Oliveira, C. G.: Gap formation and carbon cycling in the Brazilian Amazon: measurement using  
760 high-resolution optical remote sensing and studies in large forest plots. *Plant Ecol. Divers.*, 7,  
761 305–318, 2014.  
762  
763 Fauset, S., Johnson, M. O., Gloor, M., Baker, T. R., Monteagudo, A., Brienen, R. J., Feldpausch,  
764 T. R., Lopez-Gonzalez, G., Malhi, Y., Ter Steege, H. and Pitman, N. C.: Hyperdominance in  
765 Amazonian forest carbon cycling. *Nat. Commun.*, 6, 2015.  
766  
767 Fearnside, P. M.: Wood density for estimating forest biomass in Brazilian Amazonia. *Forest Ecol.*  
768 *and Manag.*, 90(1), 59-87, 1997.  
769  
770 Ferraz, A., Saatchi, S., Mallet, C., and Meyer, V.: Lidar detection of individual tree size in tropical  
771 forests. *Remote Sens. Environ.*, 183, 318-333, 2016.  
772  
773 Figueiredo, E. O., d'Oliveira, M. V. N., Braz, E. M., de Almeida Papa, D. and Fearnside, P. M.:  
774 LIDAR-based estimation of bole biomass for precision management of an Amazonian forest:  
775 Comparisons of ground-based and remotely sensed estimates. *Remote Sens. Environ.*, 187, 281-  
776 293, 2016.  
777  
778 Gentry, A. H.: *Four neotropical rainforests*. Yale University Press, 1993.  
779

780 Goldstein, G., Andrade, J. L., Meinzer, F. C., Holbrook, N. M., Cavelier, J., Jackson, P., and Celis,  
781 A.: Stem water storage and diurnal patterns of water use in tropical forest canopy trees. *Plant Cell*  
782 *Environ.*, 21(4), 397-406, 1998.

783

784 Goodman, R. C., Phillips, O. L., and Baker, T. R.: The importance of crown dimensions to improve  
785 tropical tree biomass estimates. *Ecol. Appl.*, 24(4), 680-698, 2014.

786

787 Gourlet-Fleury, S., Guehl, J.-M. and Laroussinie, O.: Ecology and management of a neotropical  
788 rainforest. Lessons drawn from Paracou, a long-term experimental research site in French  
789 Guiana. Elsevier, Amsterdam, 2004.

790 Hirata, Y.: The effects of footprint size and sampling density in airborne laser scanning to extract  
791 individual trees in mountainous terrain. Proc. ISPRS WG VIII/2 "Laser-scanners for forestry and  
792 landscape assessment", Vol. XXXVI, Part 8/W2, 3-6 October 2004, Freiburg, Germany, 2004.

793 Hopkinson, C.: The influence of flying altitude, beam divergence, and pulse repetition frequency  
794 on laser pulse return intensity and canopy frequency distribution. *Can. J. Remote Sens.*, 33(4),  
795 312-324, 2007.

796

797 Hubbell, S. P., Foster, R. B., O'Brien, S. T., Harms, K. E., Condit, R., Wechsler, B., Wright, S. J.  
798 and De Lao, S. L.: Light gap disturbances, recruitment limitation, and tree diversity in a  
799 neotropical forest. *Science*, 283, 554-557, 1999.

800

801 Jubanski, J., Ballhorn, U., Kronseder, K., Franke, J., and Siegert, F.: Detection of large above-  
802 ground biomass variability in lowland forest ecosystems by airborne Lidar. *Biogeosciences*, 10(6),  
803 3917-3930, 2013.

804

805 Kellner, J. R., and Asner, G. P.: Convergent structural responses of tropical forests to diverse  
806 disturbance regimes. *Ecol. Lett.*, 12(9), 887-897, 2009.

807

808 Laurance, W. F., Delamônica, P., Laurance, S. G., Vasconcelos, H. L., and Lovejoy, T. E.:  
809 Conservation: rainforest fragmentation kills big trees. *Nature*, 404(6780), 836-836.  
810 doi:10.1038/35009032, 2000.

811

812 Le Toan, T., Quegan, S., Davidson, M. W. J., Balzter, H., Paillou, P., Papathanassiou, K.,  
813 Plummer, S., Rocca, F., Saatchi, S., Shugart, H. and Ulander, L.: The BIOMASS mission:  
814 Mapping global forest biomass to better understand the terrestrial carbon cycle. *Remote Sens.*  
815 *Environ.*, 115(11), 2850-2860, 2011.

816

817 Lefsky, M. A., Cohen, W. B., Parker, G. G., and Harding, D. J.: Lidar remote sensing for ecosystem  
818 studies, *BioScience*, 52, 19-30, 2002.

819

820 Lefsky, M. A.: A global forest canopy height map from the Moderate Resolution Imaging  
821 Spectroradiometer and the Geoscience Laser Altimeter System. *Geophys. Res. Lett.*, 37(15), 2010.

822

823 Lefsky, M. A., Keller, M., Pang, Y., De Camargo, P. B., and Hunter, M. O.: Revised method for

824 forest canopy height estimation from Geoscience Laser Altimeter System waveforms. *J. Appl.*  
825 *Remote Sens.*, 1(1), 013537, 2007.

826  
827 Leitold, V., Keller, M., Morton, D. C., Cook, B. D., and Shimabukuro, Y. E.: Airborne Lidar-  
828 based estimates of tropical forest structure in complex terrain: opportunities and trade-offs for  
829 REDD+. *Carbon Balance Management*, 10(1), 3, 2015.

830  
831 Mascaro, J., Detto, M., Asner, G. P., and Muller-Landau, H. C.: Evaluating uncertainty in mapping  
832 forest carbon with airborne Lidar. *Remote Sens. Environ.*, 115, 3770-3774, 2011.

833  
834 Meyer, V., Saatchi, S. S., Chave, J., Dalling, J. W., Bohlman, S., Fricker, G. A., Robinson, C.,  
835 Neumann, M., and Hubbell, S.: Detecting tropical forest biomass dynamics from repeated airborne  
836 Lidar measurements. *Biogeosciences*, 10(8), 5421-5438, 2013.

837  
838 Minh, D. H. T., Le Toan, T., Rocca, F., Tebaldini, S., Villard, L., Réjou-Méchain, M., Phillips, O.  
839 L., Feldpausch, T.R., Dubois-Fernandez, P., Scipal, K. and Chave, J.: SAR tomography for the  
840 retrieval of forest biomass and height: Cross-validation at two tropical forest sites in French  
841 Guiana. *Remote Sens. Environ.*, 175, 138-147, 2016.

842  
843 Nepstad, D. C., Tohver, I. M., Ray D., Moutinho, P., and Cardinot, G.: Mortality of large trees and  
844 lianas following experimental drought in an Amazon forest. *Ecology* 88, 2259–2269, 2007.

845  
846 Nogueira, E. M., Fearnside, P. M., Nelson, B. W., and França, M. B.: Wood density in forests of  
847 Brazil's 'arc of deforestation': Implications for biomass and flux of carbon from land-use change  
848 in Amazonia. *Forest Ecol. and Manag.*, 248(3), 119-135, 2007.

849  
850 Packalen, P., Strunk, J. L., Pitkänen, J. A., Temesgen, H., and Maltamo, M.: Edge-tree correction  
851 for predicting forest inventory attributes using area-based approach with airborne laser scanning.  
852 *IEEE J. Sel. Top. Appl.*, 8(3), 1274-1280, 2015.

853  
854 Pascual, M., and Guichard, F.: Criticality and disturbance in spatial ecological systems. *Trends*  
855 *Ecol. Evol.*, 20(2), 88-95, 2005.

856  
857 Pearson, T. R., Brown, S., and Casarim, F. M.: Carbon emissions from tropical forest degradation  
858 caused by logging. *Environ. Res. Lett.*, 9(3), 034017, 2014.

859  
860 Phillips, O. L., Malhi, Y., Higuchi, N., Laurance, W. F., Núñez, P. V., Vásquez, R. M., Laurance,  
861 S. G., Ferreira, L. V., Stern, M., Brown, S. and Grace, J.: Changes in the carbon balance of tropical  
862 forests: evidence from long-term plots. *Science*, 282(5388), 439-442, 1998.

863  
864 Phillips, O. L., Aragão, L. E., Lewis, S. L., Fisher, J. B., Lloyd, J., López-González, G., Malhi, Y.,  
865 Monteagudo, A., Peacock, J., Quesada, C. A. and Van Der Heijden, G.: Drought sensitivity of the  
866 Amazon rainforest. *Science*, 323(5919), 1344-1347, 2009.

867  
868 Popescu, S. C., Wynne, R. H., and Nelson, R. F.: Measuring individual tree crown diameter with  
869 Lidar and assessing its influence on estimating forest volume and biomass. *Can. J. Remote Sens.*,

870 29(5), 564-577, 2003.  
871  
872 [Quesada, C. A., Lloyd, J., Anderson, L. O., Fyllas, N. M., Schwarz, M., and Czimczik, C. I.:](#)  
873 [Soils of Amazonia with particular reference to the RAINFOR sites, \*Biogeosciences\*, 8, 1415-](#)  
874 [1440, <https://doi.org/10.5194/bg-8-1415-2011>, 2011.](#)  
875  
876 R Core Team, 2014. R: A language and environment for statistical computing. R Foundation for  
877 Statistical Computing, Vienna, Austria. URL <http://www.R-project.org/>.  
878  
879 Réjou-Méchain, M., Tymen, B., Blanc, L., Fauset, S., Feldpausch, T. R., Monteagudo, A., Phillips,  
880 O. L., Richard, H. and Chave, J.: Using repeated small-footprint Lidar acquisitions to infer spatial  
881 and temporal variations of a high-biomass Neotropical forest. *Remote Sens. Environ.*, 169, 93-  
882 101, 2015.  
883  
884 Rocca, F., Dinh, H. T. M., Le Toan, T., Villard, L., Tebaldini, S., d'Alessandro, M. M., and Scipal,  
885 K.: Biomass tomography: A new opportunity to observe the earth forests. *Int. Geosci. Remote*  
886 *Se.*, 1421-1424, 2014.  
887  
888 Saatchi, S. S., Harris, N. L., Brown, S., Lefsky, M., Mitchard, E.T., Salas, W., Zutta, B. R.,  
889 Buermann, W., Lewis, S. L., Hagen, S. and Petrova, S.: Benchmark map of forest carbon stocks  
890 in tropical regions across three continents. *P. Natl Acad. Sci. USA*, 108(24), 9899-9904, 2011.  
891  
892 Saatchi, S. S., Asefi-Najafabady, S., Malhi, Y., Aragão, L. E., Anderson, L. O., Myneni, R. B.,  
893 and Nemani, R.: Persistent effects of a severe drought on Amazonian forest canopy. *P. Natl Acad.*  
894 *Sci. USA*, 110(2), 565-570, 2013.  
895  
896 Santiago, L. S., Goldstein, G., Meinzer, F. C., Fisher, J. B., Machado, K., Woodruff, D., and Jones,  
897 T.: Leaf photosynthetic traits scale with hydraulic conductivity and wood density in Panamanian  
898 forest canopy trees. *Oecologia*, 140(4), 543-550, 2004.  
899  
900 Simard, M., Pinto, N., Fisher, J. B., and Baccini, A.: Mapping forest canopy height globally with  
901 spaceborne lidar, *Journal of Geophysical Research - Biogeosciences*, 116, G04021,  
902 [doi:10.1029/2011JG001708](https://doi.org/10.1029/2011JG001708), 2011.  
903  
904 Slik, J. W., Paoli, G., McGuire, K., Amaral, I., Barroso, J., Bastian, M., Blanc, L., Bongers, F.,  
905 Boundja, P., Clark, C. and Collins, M. : Large trees drive forest aboveground biomass variation in  
906 moist lowland forests across the tropics. *Global Ecol. and Biogeogr.*, 22(12), 1261-1271, 2013.  
907  
908 Solé, R. V., and Manrubia, S. C.: Are rainforests self-organized in a critical state?. *J. Theor. Biol.*,  
909 173(1), 31-40, 1995.  
910  
911 Strigul, N., Pristinski, D., Purves, D., Dushoff, J., and Pacala, S.: Scaling from trees to forests:  
912 tractable macroscopic equations for forest dynamics. *Ecol. Monogr.*, 78(4), 523-545, 2008.  
913

Deleted: -

915 Ter Steege, H., Pitman, N. C., Phillips, O. L., Chave, J., Sabatier, D., Duque, A., Molino, J. F.,  
916 Prévost, M. F., Spichiger, R., Castellanos, H. and Von Hildebrand, P.: Continental-scale patterns  
917 of canopy tree composition and function across Amazonia. *Nature*, 443(7110), 444-447, 2006.  
918  
919 Ter Steege, H., Pitman, N.C., Sabatier, D., Baraloto, C., Salomão, R. P., Guevara, J.E., Phillips,  
920 O. L., Castilho, C. V., Magnusson, W. E., Molino, J. F. and Monteagudo, A. :Hyperdominance in  
921 the Amazonian tree flora. *Science*, 342(6156), 1243092, 2013.  
922  
923 Vauhkonen, J., Ene, L., Gupta, S., Heinzl, J., Holmgren, J., Pitkänen, J., Solberg, S., Wang, Y.,  
924 Weinacker, H., Hauglin, K. M. and Lien, V.: Comparative testing of single-tree detection  
925 algorithms under different types of forest. *Forestry*, 85(1), 27-40, 2011.  
926  
927 Vauhkonen, J., Næsset, E., and Gobakken, T.: Deriving airborne laser scanning based  
928 computational canopy volume for forest biomass and allometry studies. *ISPRS J. Photogramm.*,  
929 96, 57-66, 2014.  
930  
931 Vincent, G., Sabatier, D., Blanc, L., Chave, J., Weissenbacher, E., Pélissier, R., Fonty, E., Molino,  
932 J. F. and Couteron, P.: Accuracy of small footprint airborne Lidar in its predictions of tropical  
933 moist forest stand structure. *Remote Sens. Environ.*, 125, 23-33, 2012.  
934  
935 West, G.B., Enquist, B. J. and Brown, J. H. : A general quantitative theory of forest structure and  
936 dynamics. *P. Natl Acad. Sci. USA*, 106, 7040–7045, 2009.  
937  
938 Zhou, J., Proisy, C., Descombes, X., Hedhli, I., Barbier, N., Zerubia, J., Gastellu-Etchegorry, J.  
939 P. and Couteron, P.: Tree crown detection in high resolution optical and Lidar images of tropical  
940 forest. *P. Soc. Photo-Opt. Ins.*, 7824. SPIE, 2010.  
941 , 2010.  
942  
943

944  
 945  
 946  
 947  
 948  
 949  
 950  
 951

**Table 1.** Information on forest inventory plots. \* indicates that a site has been used for the calibration of the LCA model. Sources: Antimary and Cotriguaçu: Fearnside, 1997; d'Oliveira et al., 2012, BCI: Center for Tropical Forest Science (CTFS) (Condit, 1998; Hubbell et al., 1999, 2005), Chocó: ([bioredd.org](http://bioredd.org)), La Selva: Carbono project (Clark and Clark, 2000), Manaus and Tapajós: Espírito-Santo (unpublished results), Nouragues: Réjou-Méchain et al., 2015, Paracou: Gourlet-Fleury et al., 2004; Vincent et al., 2012.

Site	Data	Plots Size (ha)	N plots	Year	Mean WD (g cm <sup>-3</sup> )	Mean AGB (Mg ha <sup>-1</sup> )	Annual rainfall (mm yr <sup>-1</sup> )
Antimary (Brazil)	Plot level	0.25	50	2010	0.61	234	2000
BCI* (Panama)	Tree level	1	50	2010	0.56	235	2600
Chocó (Colombia)	Tree level	0.25	42	2013	0.60	224	10000
Cotriguaçu (Brazil)	Not available	-	-	-	0.60	-	2000
La Selva* (Costa Rica)	Tree level	1	11	2009	0.45	178	4000
Manaus (Brazil)	Tree level	0.25	10	2014	0.66	263	2200
Nouragues* (French Guiana)	Plot level	1	33	2012	0.66	424	3000
	Tree level	1	7/33				
Paracou* (French Guiana)	Plot level	1	85	2009-10	0.71	353	3000
Tapajós (Brazil)	Tree level	0.25	10	2014	0.62	238	1900

952

953



954 **Table 2.** Information on Lidar data and locations of the 9 research sites.

Site	Sensor	Year	Retur	Flight	Scanning	Frequency	NW corner lat	NW corner lon
(1km <sup>2</sup> images)			ns m <sup>2</sup>	Altitude (m)	angle (°)	(kHz)		
<b>Antimary</b>	Optech ALTM3100EA	2010-2011	10-15	500	11	70	9°17'47.26"S	68°17'15.06"W
<b>BCI</b>	Optech ALTM3100EA	2009	8	1000	35	70	9°9'28.56"N	79°51'18.9"W
<b>Chocó</b>	Optech ALTM3033	2013	4	1000	20	33	3°57'5.71"N	76°49'10.31"W
<b>Cotriguaçu</b>	Optech ALTM3100EA	2011	10-15	850	11	60	9°27'8.87"S	58°51'51.22"W
<b>La Selva</b>	Optech ALTM3100EA	2009	4	1500	20	70	10°25'37.97"N	84°18.76"W
<b>Manaus</b>	Optech ALTM3100EA	2012	10-15	850 (max)	11	60	2°56'38.48"S	59°56'12.57"W
<b>Nouragues</b>	Riegl LMS-Q560	2012	12	400	45	200	4°3'10.0"N	52°42'19.95"W
<b>Paracou</b>	Riegl LMS-280i	2009	4	120-220	30	24	5°15'47.73"N	52°56'26.96"W
<b>Tapajós</b>	Optech ALTM3100EA	2011	10-15	850 (max)	11	60	2°50'53.41"S	54°57'44.53"W

955

956

957  
958

**Table 3.** Coefficients,  $R^2$ , RMSE and bias for the models used to estimate  $AGB_{LCA}$  without and with wood density as a weighting factor ( $m_{LCA}$ ) and  $m_{LCA\_wd}$ , respectively).

Model	Equation	a	b	$R^2$	RMSE	Bias	$R^2$ cross-val	RMSE cross-val	Bias cross-val
$m_{LCA}$	$AGB = aLCA + b$ (Eq. (2))	3.56	136.91	0.59	62.53	0.0	0.58	63.26	0.16
$m_{LCA\_wd}$	$AGB = (aLCA+b) \times WD$ (Eq. (3))	4.47	270.27	0.78	46.02	-0.76	0.77	46.47	-0.63

959  
960

|

961

962 **Figure 1.** Segmentation of the 1 km × 1 km images in each site using five canopy height thresholds. A minimum of  
963 100 contiguous pixels was used as a segmentation threshold in all cases.

964 **Figure 2.** LCA in function of height thresholds in the nine study sites. The steepest slopes are between 24 m  
965 (Antimary) and 30 m (Nouragues), with an average of 27 m across sites. Steepness of slope was obtained by calculating  
966 the derivative of the sigmoid models characterizing each site.

967 **Figure 3.** Distribution of R<sup>2</sup> between tree height thresholds used to determine LCA and  $AGB_{local}$  in the nine 1 ha  
968 subareas (a) and distribution of R<sup>2</sup> between tree height thresholds and  $AGB_{inv}$  in 1 ha inventory plots of the four  
969 calibration sites (b). All optimal thresholds are between 23 m and 30 m. The average maximal height threshold is 27  
970 m.

971 **Figure 4.** Relationship between  $AGB_{inv}$  and LCA (a),  $AGB_{inv}$  normalized by averaged wood (b), and  $AGB_{inv}$  vs.  
972  $AGB_{LCA}$  estimated with LCA\_wd model (c). The black line represents the 1-to-1 line. Normalizing AGB by averaged  
973 wood density brings the data from different sites closer to a common fit.

974 **Figure 5.**  $AGB_{MCH}$  vs.  $AGB_{LCA}$  in the plots of the four calibration sites (a), and  $AGB_{MCH}$  vs.  $AGB_{LCA}$  in the 1km<sup>2</sup>  
975 images of the nine sites (b). The black line represents the 1-to-1 line.

976 **Figure 6.** Detection of changes of forest structure from selective logging in the Antimary study area showing a) the  
977 difference between pre- and post- logging (2010–2011) Lidar derived LCA at 1 ha grid cells over the entire study area,  
978 b) the histogram of LCA for the two Lidar datasets showing the mean difference and the reduction of medium and  
979 large LCA areas from selective logging, c) 2010 Lidar LCA segmentation at 1 m resolution over a sample area in the  
980 north of the study site, d) same LCA segmentation for 2011 Lidar data, and e) difference of the two segmented areas  
981 showing the extent of the logging impact on large trees in addition to natural changes of forest structure from changes  
982 in canopy gaps from tree falls and tree growth.

983 **Figure 7.** Relationship between LCA and  $AGB_{LCA}$  (a) and relationship between  $AGB_{inv}$  of large trees (>50 cm DBH)  
984 and total  $AGB_{inv}$  (b). In both cases, the intercepts represent the contribution of small trees to total AGB. Note that  
985 Manaus and Nouragues overlap because they have the same mean wood density, as well as Chocó and Cotriguaçu.  
986  
987  
988

993

994

Deleted:  $AGB_{Lidar}$

Deleted: density

Deleted: and

Deleted: AGB

Deleted: density

Deleted: .

Deleted:  $AGB_{inv}$

Deleted: density

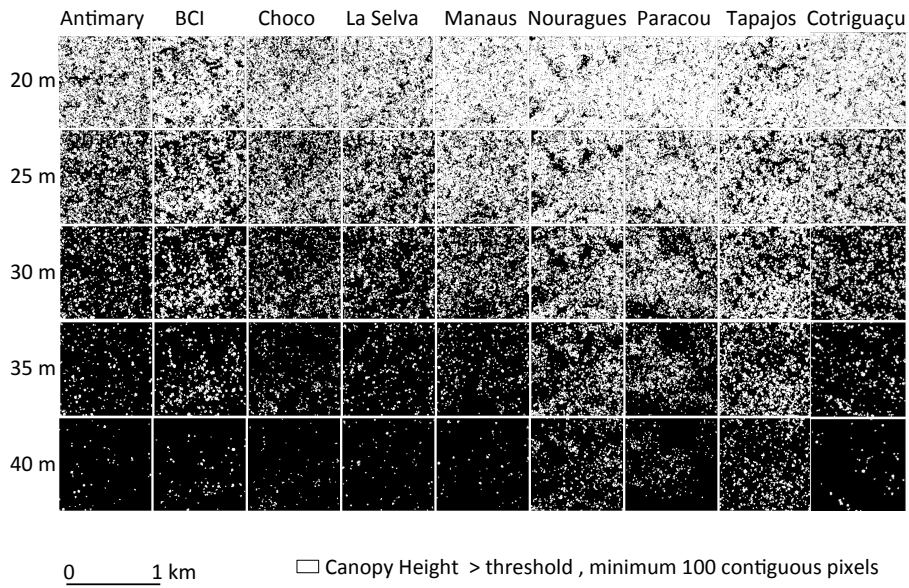
Deleted: estimated with LCA\_wd model

Deleted: .

Formatted: Superscript

Deleted:  $AGB_{Lidar}$  density from the 1km<sup>2</sup> images vs.  $AGB_{LCA}$  estimated with LCA\_wd model (b).

1007 Figure 1

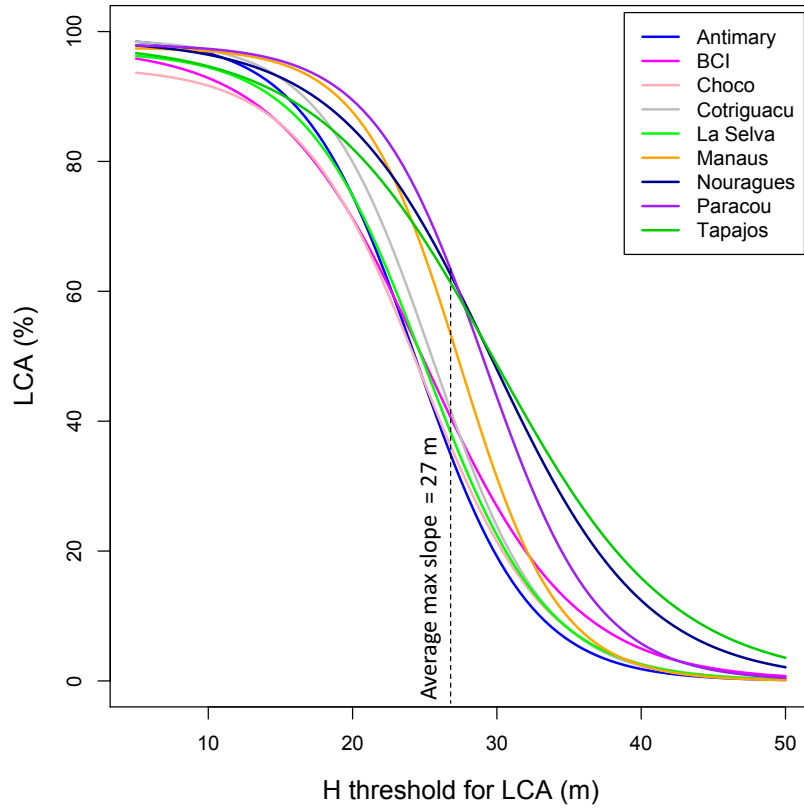


1008

1009

|

1010 Figure 2

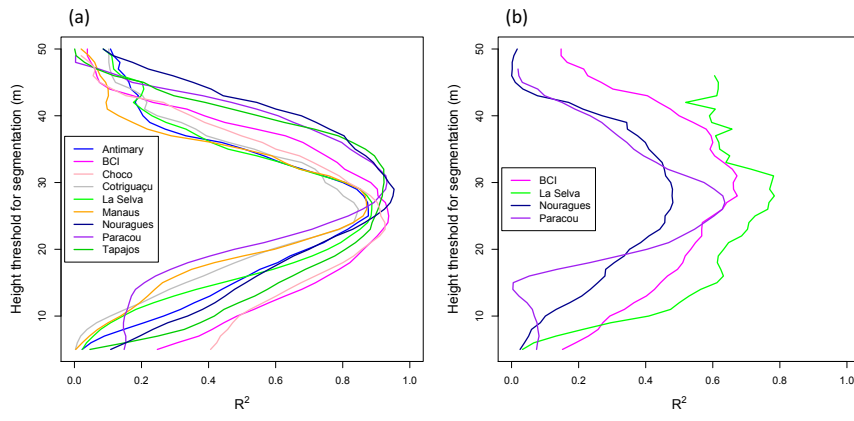


1011

1012

|

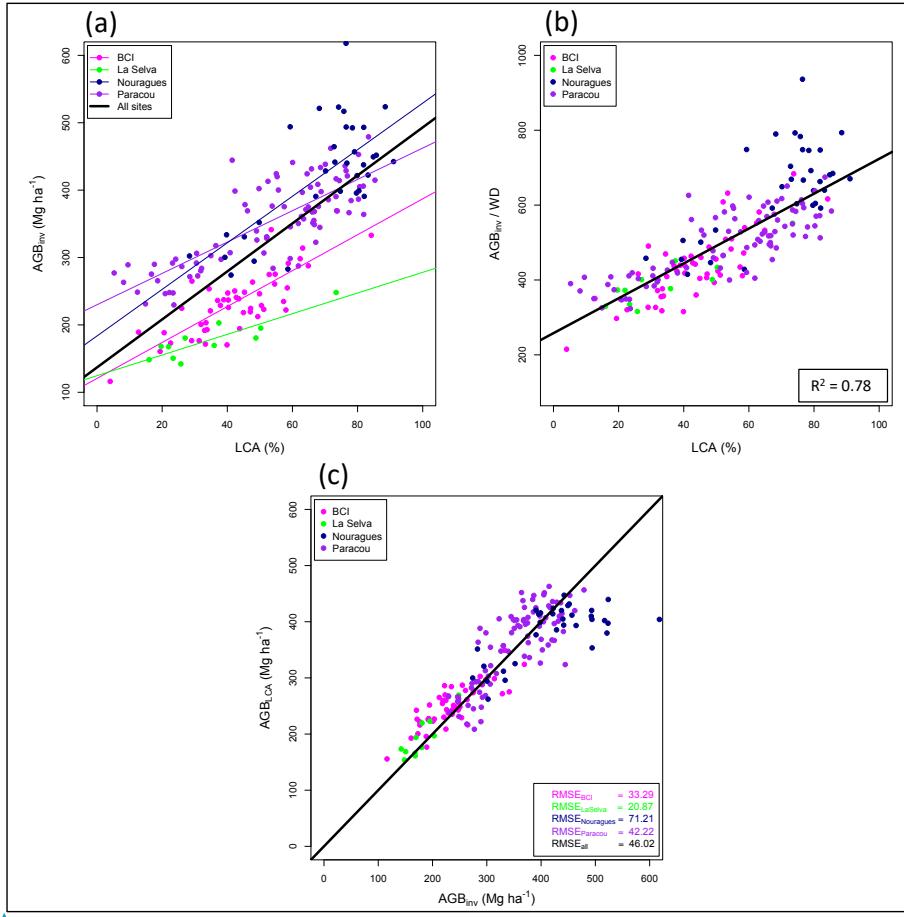
1013 Figure 3



1014

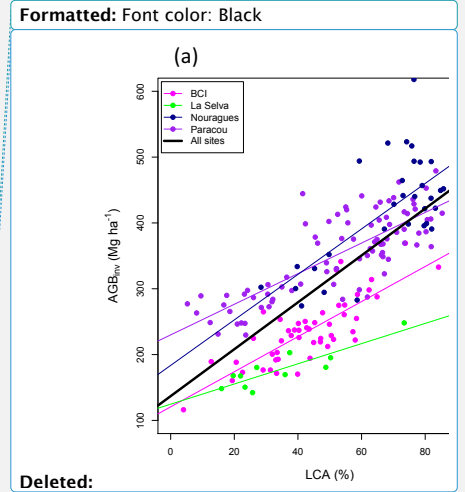
1015

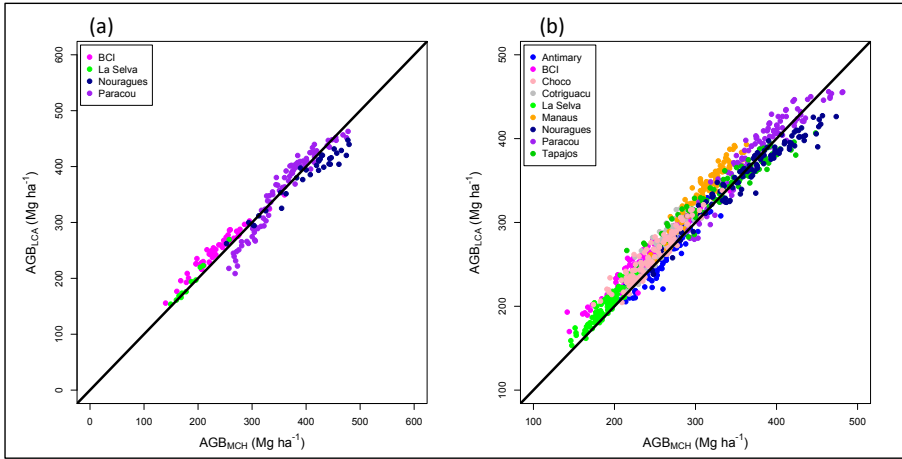
|



1017

1018

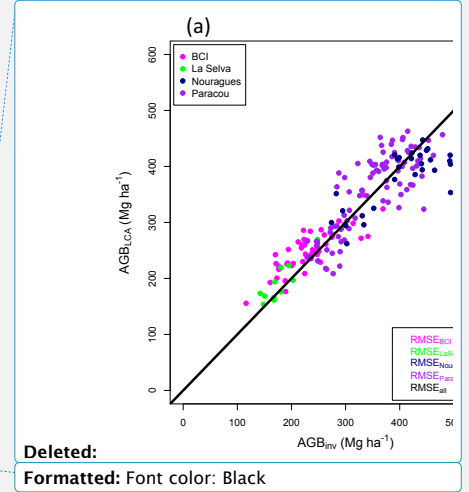




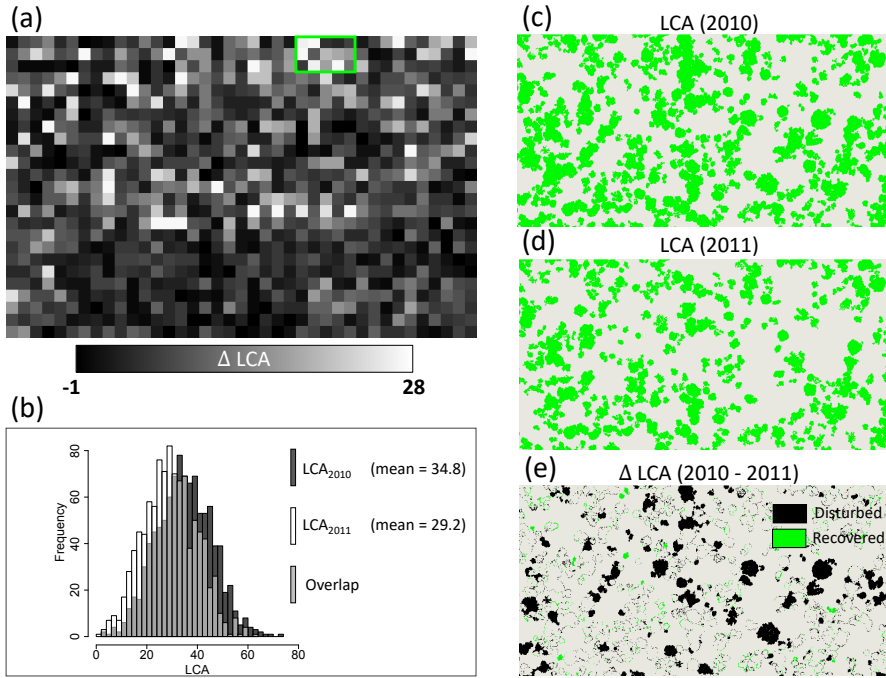
1021

1022

1023

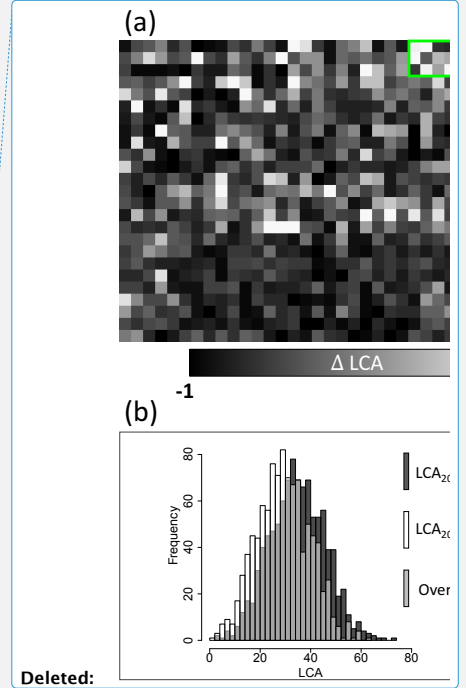






1026

1027



|

